# Zinc-binding triggers a conformational-switch in the cullin-3 substrate adaptor protein KEAP1 that controls transcription factor NRF2

McMahon, Michael; Swift, Samuel R.; Hayes, John D.

*Published in:*
Toxicology and Applied Pharmacology

*DOI:*
10.1016/j.taap.2018.09.033

*Publication date:*
2018

Elsevier Editorial System(tm) for Toxicology and Applied Pharmacology

Manuscript Draft

Manuscript Number: TAAP-D-18-00741R1

Title: ZINC-BINDING TRIGGERS A CONFORMATIONAL-SWITCH IN THE CULLIN-3 SUBSTRATE ADAPTOR PROTEIN KEAP1 THAT CONTROLS TRANSCRIPTION FACTOR NRF2

Article Type: VSI: Nrfs in Tox & Pharmacol

Keywords: NRF2;
KEAP1;
Zinc;
Danger signal;
Ubiquitylation

Corresponding Author: Dr. Michael John McMahon, Ph.D.

Corresponding Author's Institution: Concept Life Sciences

First Author: Michael John McMahon, Ph.D.

Order of Authors: Michael John McMahon, Ph.D.; Samuel R Swift, PhD; John D Hayes, PhD

Abstract: Kelch-like ECH-associated protein 1 (Keap1) is a cullin-3 (Cul3)-RING ubiquitin ligase (CRL) adaptor/scaffold protein that enables cells to adapt to environmental stressors because modification of certain of its Cys residues initiates de-repression of the NF-E2 p45-related factor-2 (Nrf2) transcription factor. Thus, in normal unstressed cells, the cytoprotective Nrf2 is continuously ubiquitylated by CRLKeap1, thereby ensuring that Nrf2 is efficiently degraded by the proteasome and expression of Nrf2 target genes restricted. By contrast, this process is attenuated in stressed cells, allowing Nrf2 protein to accumulate in the nucleus and induce genes that promote cell survival. It remains unclear how Keap1 senses stress. Previously, we suggested that release of free Zn2+ from damaged proteins represents an endogenous 'danger' signal recognized by Keap1. However, the existence of a Zn2+ sensor in Keap1 is not widely acknowledged. We now present data that support the hypothesis that Keap1 directly senses Zn2+ through a cluster of amino-acids that include His-225, Cys-226, and Cys-613. We show that this mechanism does not require p62/sequestosome-1, an autophagy adaptor protein implicated in metal(loid) sensing by Keap1. Moreover, using a genetically-encoded FRET reporter, we present evidence that binding of Zn2+ triggers a conformational switch in Keap1. The altered conformation of Keap1 is envisaged to perturb the architecture of CRLKeap1, such that bound Nrf2 becomes mis-aligned with respect to the ubiquitin-charged E2 enzyme. These data are consistent with the notion that Keap1 possesses a Zn2+ sensor whose triggering distorts its structure of in a fashion that inhibits ubiquitylation of Nrf2 upon CRLKeap1.

## HIGHLIGHTS

- Keap1 acts as a sensor for intracellular zinc
- Keap1 senses zinc through co-ordination chemistry
- Binding of zinc by Keap1 is accompanied by a conformational change
- The conformational change in Keap1 arrests ubiquitylation of Nrf2

# ZINC-BINDING TRIGGERS A CONFORMATIONAL-SWITCH IN THE CULLIN-3 SUBSTRATE ADAPTOR PROTEIN KEAP1 THAT CONTROLS TRANSCRIPTION FACTOR NRF2

**Michael McMahon[a,c,1], Samuel R. Swift[b], and John D. Hayes[a,1]**

*[a]Division of Cancer Research, School of Medicine, Ninewells Hospital and Medical School, University of Dundee, Dundee DD1 9SY; [b]MSI/WTB/JBC complex, College of Life Sciences, University of Dundee, Dundee DD1 4HN, Scotland, United Kingdom; c Current address: Concept Life Sciences, Dundee DD1 5JJ, Scotland, United Kingdom*

[1]Corresponding authors: John D. Hayes,

Tel: +44 1382 383182

j.d.hayes@dundee.ac.uk

Michael McMahon

Tel: +44 1382 432163

Michael.Mcmahon@conceptlifesciences.com

**ABSTRACT**

Kelch-like ECH-associated protein 1 (Keap1) is a cullin-3 (Cul3)-RING ubiquitin ligase (CRL) adaptor/scaffold protein that enables cells to adapt to environmental stressors because modification of certain of its Cys residues initiates de-repression of the NF-E2 p45-related factor-2 (Nrf2) transcription factor. Thus, in normal unstressed cells, the cytoprotective Nrf2 is continuously ubiquitylated by $CRL^{Keap1}$, thereby ensuring that Nrf2 is efficiently degraded by the proteasome and expression of Nrf2 target genes restricted. By contrast, this process is attenuated in stressed cells, allowing Nrf2 protein to accumulate in the nucleus and induce genes that promote cell survival. It remains unclear how Keap1 senses stress. Previously, we suggested that release of free $Zn^{2+}$ from damaged proteins represents an endogenous 'danger' signal recognized by Keap1. However, the existence of a $Zn^{2+}$ sensor in Keap1 is not widely acknowledged. We now present data that support the hypothesis that Keap1 directly senses $Zn^{2+}$ through a cluster of amino-acids that include His-225, Cys-226, and Cys-613. We show that this mechanism does not require p62/sequestosome-1, an autophagy adaptor protein implicated in metal(loid) sensing by Keap1. Moreover, using a genetically-encoded FRET reporter, we present evidence that binding of $Zn^{2+}$ triggers a conformational switch in Keap1. The altered conformation of Keap1 is envisaged to perturb the architecture of $CRL^{Keap1}$, such that bound Nrf2 becomes mis-aligned with respect to the ubiquitin-charged E2 enzyme. These data are consistent with the notion that Keap1 possesses a $Zn^{2+}$ sensor whose triggering distorts its structure of in a fashion that inhibits ubiquitylation of Nrf2 upon $CRL^{Keap1}$.

**KEYWORDS**: NRF2, KEAP1, Zinc, Danger signal, Ubiquitylation

## ABBREVIATIONS

4HNE: 4-hydroxynon-2-enal; Acro: acrolein; tBHQ: *tert*-butyl hydroquinone; Sul: sulforaphane; ZnPy: $Zn^{2+}$-pyrithione complex

## INTRODUCTION

Cells have evolved mechanisms that maintain their structural integrity despite unpredictable and deleterious alterations in their immediate environment (Kitano, 2004) . For example, they adapt to adverse circumstances by re-wiring metabolism, re-programming gene expression and attenuating protein translation. It is well established that in cells exposed to pro-oxidant or electrophilic xenobiotics, a battery of genes is induced that encodes detoxication- and antioxidant enzymes, as well as other proteins involved in the removal and repair of damaged macromolecules (Gasch, 2007; Hayes and Dinkova-kostova, 2014; Hecker et al., 2007; Hengge-Aronis, 1999; Kültz, 2004). In bilateran species, this adaptation to oxidants and electrophilic stressors is orchestrated by Kelch-like ECH-associated protein 1 (Keap1), a substrate adaptor for the cullin-3 (Cul3)-RING ubiquitin ligase (CRL). Specifically, the $CRL^{Keap1}$ complex is able to perceive 'danger' and/or 'damage' signals, and in so doing adjusts accordingly the stability of NF-E2 p45-related factor 2 (Nrf2), a cap'n'collar (CNC) basic-region leucine zipper (bZIP) transcription factor that directs expression of antioxidant proteins, NADPH generating enzymes, drug-metabolizing enzymes and drug-efflux pumps (McMahon et al., 2010; Yamamoto et al., 2018).In model organisms, the consequences of a failure to mount this adaptive response are stark; they include accelerated onset and increased severity of degenerative diseases, afflicting all major organs (Kensler et al., 2007; Sykiotis and Bohmann, 2010) .

The $CRL^{Keap1}$ complex, as modelled in **Fig S1A-C**, comprises the Cul3-RING-box 1 (Rbx1) holoenzyme and the dimeric substrate adaptor/scaffold protein Keap1 (Canning et al., 2013) . Critically, Keap1, which typically comprises 624 amino acids in

mammalian species, contains a Broad complex, Tramtrack, and Bric-à-brac (BTB) domain between residues 50 and 184 that recruits Cul3, and a Kelch-repeat domain between residues 327 and 611 that binds Nrf2 (Canning et al., 2015) . Molecular modeling, mutagenesis (McMahon et al., 2006) and NMR studies (Kit I Tong et al., 2006) suggest that $CRL^{Keap1}$ ubiquitylates Nrf2 through a two-site binding process in which each of the two Kelch-repeat domains in the complex interacts with either a high-affinity ETGE motif or a low-affinity DLG motif within the Nrf2-ECH homology 2 (Neh2) domain of the CNC-bZIP transcription factor (**Fig S1D**). Two-site docking of a single Nrf2 polypeptide upon $CRL^{Keap1}$ is believed to immobilize a nine-turn α-helix that lies between the ETGE- and DLG motifs. Consequently, seven lysine residues lying on one face of this α-helix become juxtaposed with the Rbx1-bound Ub~E2 enzyme and ubiquitylation of Nrf2 ensues (McMahon et al., 2006; Zhang et al., 2004) ; this confers a short half-life of approximately only 5-20 min on the CNC-bZIP protein in healthy unstressed cells (McMahon et al., 2003) . However, in response to exposure to potentially injurious agents, $CRL^{Keap1}$ becomes less efficient at ubiquitylating Nrf2, allowing the CNC-bZIP transcription factor to accumulate in the nucleus, where it dimerizes with a small musculoaponeurotic fibrosarcoma (Maf) protein, and transactivates cytoprotective and other genes that contribute to adaptation to stress (Kensler et al., 2007) .

The ability of $CRL^{Keap1}$ to target Nrf2 for proteasomal degradation is influenced by nutritional status of the cell and is increased by O-GlcNAcylation at Ser-104, catalysed by O-GlcNAc transferase (Chen et al., 2017) . By contrast with the positive effects glycosylation of Keap1 has on the activity of $CRL^{Keap1}$, the mechanisms by which

93 Keap1 perceives stress and attenuates $CRL^{Keap1}$ activity are not well understood (Holland
94 and Fishbein, 2010) . This is particularly true of the ability of Keap1 to recognise
95 endogenous 'danger' signals, which we imagine would have been of evolutionary
96 significance. Since its discovery in 1999 (Itoh et al., 1999) , it has become widely
97 accepted that the principal mechanism by which Keap1 recognizes pro-oxidants and
98 electrophiles involves a limited number of critical cysteine-based sensors (Dinkova-
99 Kostova et al., 2002; Hourihan et al., 2012; Jain et al., 2010; Saito et al., 2016; Zhang and
100 Hannink, 2003) . In particular, mouse and human Keap1 proteins contain 25 and 27 Cys
101 residues, respectively, and amongst these Cys-151, Cys-273 and Cys-288 are widely
102 conserved between mammalian species and appear to contribute to the sensing of
103 endogenous 'danger' signals. The signalling molecule nitric oxide (NO) represents one
104 such 'danger' signal (McMahon et al., 2010; Zhang and Hannink, 2003) , and it is
105 recognized by Keap1 through nitrosation of its Cys-151 that resides in the BTB domain.
106 By contrast, the alkenals 4-hydroxynon-2-enal (4HNE) and acrolein (Acro), which are
107 frequently produced by damaged cells as a consequence of lipid peroxidation (Dargel,
108 1992) , represent another class of endogenous 'danger' signal. These lipid-derived α,β-
109 unsaturated aldehydes, are recognized by a sensor(s) within Keap1 that involves *S*-
110 alkylation of Cys-273 and/or Cys-288 within the intervening region (IVR) (McMahon et
111 al., 2010; Saito et al., 2016) , which is located between residues 209 and 314. Itaconate
112 is another example of an endogenous α,β-unsaturated aldehyde, which is produced by
113 macrophages as an anti-inflammatory response to lipopolysaccharide and could be
114 regarded as a 'danger' signal; in this case, itaconate interacts with Keap1 at Cys-273 and
115 Cys-288 as well as other Cys residues (Mills et al., 2018) . A yet further class of

116 ‘danger’ signal may include hydrogen sulphide (Hourihan et al., 2012) and hydrogen
117 peroxide (Fourquet et al., 2010) , for which Keap1 has been postulated to have
118 additional sensors. Besides allowing Keap1 to recognize endogenous ‘danger’ signals,
119 Cys-151, Cys-273, and Cys-288 also recognize directly some common environmental
120 toxins (see **Fig 1A**) (McMahon et al., 2010) .

121 Besides the two prototypic Keap1 signaling pathways that are triggered by
122 chemical modification of Cys-151 or Cys-273/Cys-288, an additional mechanism by
123 which Nrf2 may be stabilized is the so-called “non-canonical pathway” that involves
124 p62/sequestosome-1, an adaptor/scaffold that recruits specific cargos for selective
125 autophagy (Katsuragi et al., 2016) . In this “non-canonical pathway”, p62 is
126 phosphorylated at the Ser residue in a STGE motif by mechanistic target of rapamycin
127 complex 1 (mTORC1), with the post-translationally modified pSTGE-containing form of
128 p62 resembling the ETGE motif in Nrf2, thereby enabling p62 to inhibit competitively
129 the binding of the CNC-bZIP transcription factor to Keap1 under circumstances when
130 mTORC1 is active (Ichimura et al., 2013) . As a consequence of the competition
131 between binding of Nrf2 and phosphorylated p62 for Keap1, conditions that induce
132 selective autophagy also result in stabilisation of Nrf2. Conversely, p62 itself is degraded
133 during this process and therefore conditions that inhibit selective autophagy, such as
134 treatment with arsenite, cause p62 to accumulate with the net effect of stabilizing Nrf2
135 (Lau et al., 2013) .

136 We previously suggested that $Zn^{2+}$ represents an additional ‘danger’ signal
137 recognized by Keap1 directly through co-ordination chemistry involving His-225, Cys-
138 226, and Cys-613 (McMahon et al., 2010) . Zinc is well-placed for such a role as it is

139 released from damaged proteins (Eide, 2006) and may also be mobilized from
140 specialized vesicles in response to injury (Abiria et al., 2017) . However, the role of
141 $Zn^{2+}$ as a 'danger' signal has received relatively little attention and the notion that
142 collectively His-225/Cys-226/Cys-613 comprise a further stress sensor that functions
143 independently of Cys-151 and Cys-273/Cys-288 has not gained traction in the scientific
144 literature. It also remains unclear how endogenous 'danger' signals, including $Zn^{2+}$,
145 reduce the rate at which Nrf2 is ubiquitylated by $CRL^{Keap1}$. Earlier studies led to the
146 proposal that in stressed cells disassembly of the Nrf2-$CRL^{Keap1}$ complex accounts for
147 Nrf2 stabilization (Hayes and McMahon, 2009) . Most commonly, it was proposed that
148 in stressed cells the Nrf2-Keap1 interaction became disrupted (Itoh et al., 1999) , but it
149 has also been proposed that passive dissociation of Keap1 from the Cul3-Rbx1
150 holoenzyme (Eggler et al., 2009; Rachakonda et al., 2008; Zhang et al., 2004) or active
151 degradation of Keap1 (Hong et al., 2005; Zhang et al., 2005) may account for the
152 increase in Nrf2 activity. However, this disassembly model remains controversial and
153 there is now compelling evidence that the Nrf2 continues to interact with Keap1 in
154 stressed cells (Baird et al., 2013) .

155 We now report data confirming that free $Zn^{2+}$ is recognized by Keap1 through co-
156 ordination chemistry involving a limited number of amino acids, of which the most
157 important are His-225, Cys-226, and Cys-613. We show that the Nrf2-$CRL^{Keap1}$ complex
158 persists in cells treated with chemicals that trigger any of the NO, alkenal, and $Zn^{2+}$
159 sensors. Moreover, we present evidence that the $Zn^{2+}$ sensor operates as a conformational
160 switch that distorts the domain architecture of Keap1 and, consequently, mis-aligns the
161 relative positioning of the CNC-bZIP factor and the Rbx1-bound ubiquitin-charged E2

conjugating (Ub~E2) enzyme. Collectively, our data suggest a hitherto undocumented molecular mechanism that controls the activity of $CRL^{Keap1}$ towards Nrf2, which might be used more generally for controlling the activity of this class of ubiquitin ligase.

## METHODS

*Chemicals*

Acrolein (Acro), 4-hydroxynon-2-enal (4HNE), *tert*-butyl hydroquinone (tBHQ), $CdCl_2$ ($Cd^{2+}$), $ZnCl_2$ ($Zn^{2+}$), $NaAsO_2$ ($As^{3+}$), $Na_2SeO_3$ ($Se^{4+}$), pyrithione, and cycloheximide (CHX) were purchased from Sigma-Aldrich UK. Sulforaphane (Sul) was obtained from LKT laboratories (St Paul, MN, USA). MG132 was supplied by Calbiochem. Vehicles, stock solutions, and final concentrations of all chemicals (unless explicitly stated otherwise in the text) are summarized in **Table 1**. Zinc-pyrithione complexes (0.5 mmol/l) were prepared fresh before use by adding 16.6 μl of pyrithione stock solution to 1 ml of MilliQ water, vortexing, and then adding 3.3 μl of the $ZnCl_2$ stock solution. Final concentrations of Zinc-pyrithione varied and are specified in the text.

*Cell culture, transfections, chemical challenge and β-galactosidase assay*

Immortalized *Keap1*$^{-/-}$ mouse embryonic fibroblast (MEF) cells (and wild-type controls) were a kind gift from Prof. Masayuki Yamamoto (Tohoku University, Japan). The *p62*$^{-/-}$ MEF cells and corresponding wild-type controls were a kind gift from Prof. Masaaki Komatsu (Niigata University, Japan). COS1 and MEF cells were cultured and transfected as described previously (McMahon et al., 2006, 2003) . The cultured cells were challenged with chemicals not less than 24 h after plating.

*Plasmids*

The pKeap1FRET plasmid employed in this project expresses a mCerulean-mKeap1$^{\Delta Kelch}$-mEYFP fusion protein (Keap1FRET) and was generated in four stages. Firstly, pmCerulean-C1 was derived by site-directed mutagenesis (SDM) from pECFP-C1 and it expresses a variant form of ECFP that contains the amino acid substitutions S72A, Y145A and H148D to enhance the quantum yield of the protein (generating the Cerulean variant of ECFP), as well as an A206K substitution to generate a monomeric (m) form of the protein. Secondly, pmEYFP-N1 was derived by SDM from pEYFP-N1 and expresses a monomeric form of EYFP that bears an A206K amino acid substitution. Thirdly, a fragment of the cDNA for mouse Keap1 (encoding amino acids 1-327) that lacks the Kelch-repeat domain was amplified by PCR using the forward primer 5′-CTGTGTCTTGTCATCCGGACTCGAGTGCAGCCCGAACCCAAGCTTAGC-3′ and the reverse primer 5′-GAAGTAACCGCCCGCTGTGGGATCCAGGCGGCCTACTTTGGGCGC-3′ with restriction sites underlined. The resulting product was digested with XhoI and BamHI and ligated into similarly-digested pmEYFP-N1. Finally, the mouse Keap1$^{\Delta Kelch}$-mEYFP-encoding sequence from the resulting recombinant plasmid was excised using XhoI and XbaI and ligated into similarly-digested pmCerulean-C1 to generate pKeap1FRET. The pHisMycRbx1 plasmid, which encodes his-Myc-Rbx1, was a kind gift from Prof. Joan

207 Conaway, Stowers Research Institute, Kansas City, USA (Kamura et al., 1999) . All
208 remaining plasmids have been described previously (McMahon et al., 2006, 2003) .
209
210
211 *Immunoblots and immunoprecipitations*
212 For immunoblots, whole-cell lysates were prepared by scraping cell monolayers into ice-
213 cold radioimmune precipitation assay buffer (50 mM Tris-Cl, pH 7.4, 150 mM NaCl, 1%
214 (v/v) Nonidet P-40, 0.5% (w/v) deoxycholic acid, 0.1% (w/v) SDS that was
215 supplemented with complete, EDTA-free protease inhibitor mixture (Roche Applied
216 Science)). Lysates were clarified by centrifugation (16,000 x *g*, 15 min, 4$^{o}$C). Protein
217 determination, SDS/polyacrylamide-gel electrophoresis and immunoblotting were carried
218 out using standard methods (McMahon et al., 2003) . Antibodies used, and the
219 concentrations employed were as follows: affinity-purified antiserum against mNrf2 that
220 was isolated using conventional techniques, 0.02 μg/ml (McMahon et al., 2003) ;
221 affinity-purified rabbit antibodies against mKeap1 (McMahon et al., 2006) , 0.05 μg/ml;
222 mouse anti-V5 (Invitrogen), 0.5 μg/ml; mouse anti-myc clone 9E10 (Abcam), 0.5 μg/ml;
223 rabbit anti-GFP (Abcam), 0.5 μg/ml; mouse anti-actin (Sigma), 0.1 μg/ml; guinea-pig
224 anti-mouse p62 (Progen), 0.1 μg/ml. Immunoprecipitation of endogenous Keap1, EGFP-
225 or V5-tagged proteins from clarified, whole-cell lysates was performed by conventional
226 methods. Briefly, clarified whole-cell lysates were prepared as described above for
227 immunoblotting, except that deoxycholic acid and SDS were omitted from the
228 radioimmune precipitation assay buffer. A 50 μl aliquot of Protein G-Sepharose 4B
229 (Sigma) was washed with the modified radioimmune precipitation assay buffer, by

repeated centrifugation (5,000 x *g*, 2 min, 4 $^{o}$C). The clarified lysate was added to the washed resin along with 0.125 μg of rabbit anti-mKeap1, rabbit anti-GFP or mouse anti-V5 and the suspension was mixed by end-over-end tumbling at 4 $^{o}$C for 2 h. Thereafter, the resin was washed with three volumes of modified radioimmune precipitation assay buffer, by repeated centrifugation (5,000 x *g*, 2 min, 4 $^{o}$C). Material that remained bound to the resin was eluted in 50 μl of Laemmli SDS sample buffer, reducing (with 2-mercaptoethanol).

*Light microscopy and immunocytochemistry*

Cells were grown and transfected on 0.17-mm thick, ethanol-washed glass coverslips. They were fixed by treatment with a 4% (w/v) solution of paraformaldehyde in PBS for 10 min at room temperature and permeabilised with a 0.2% (v/v) solution of Triton X-100 in PBS, also for 10 min at room temperature. Cells were blocked by immersion in a 5% (v/v) solution of fetal bovine serum in PBS for 40 min at 4$^{o}$C. The fixed and blocked samples were incubated with primary antibodies (mouse anti-V5 (Invitrogen) to detect V5-tagged proteins; affinity-purified rabbit anti-mNrf2 antibodies (McMahon et al., 2003) to detect endogenous mNrf2; mouse anti-human p62 (BD Biosciences) to detect p62) at 10 μg/ml in blocking buffer, for 1 h at 4$^{o}$C. Subsequently, the primary antibodies were detected using a 10 μg/ml solution of either Alexa Fluor 568-conjugated goat anti-mouse IgG, or Alexa-Fluor 488-conjugated goat anti-rabbit IgG (Molecular Probes) in blocking buffer, for 1 h at 4$^{o}$C. To stain DNA, TO-PRO-3 (Molecular Probes) was included in this secondary antibody solution at a final concentration of 1 μg/ml. To stain filamentous actin, Texas Red-X-conjugated phalloidin (Molecular Probes) was also

included in the secondary antibody solution at a final concentration of 16.5 nmol/l. Coverslips were mounted on glass slides using Mowiol mounting medium (0.1 M Tris, pH 8.5, 10% (w/v) Mowiol 4-88, 25% (v/v) glycerol and 10 μg/ml 1,4-diazabicyclo(2,2,2)octane (DABCO)). Specimens were viewed using the LSM 510 confocal microscope (Zeiss) with a 40x or a 63x PlanApochromat objective. Fluorescent signals of EGFP or Alexa Fluor 488 (excitation 488 nm using an Ar laser), Texas Red-X or Alexa Fluor 568 (excitation 543 nm using a HeNe1 laser) and TO-PRO-3 (excitation 633 nm using a HeNe3 laser) were detected using band-pass 505-530 nm, 560-615 nm and long-pass 650 nm emission filters, respectively.

*In vivo crosslinking of proteins followed by purification of his-tagged protein*

COS1 cells in 60-mm dishes were co-transfected with plasmids encoding mKeap1-V5-his and the protein whose interaction with Keap1 was under investigation. After 24 h, a 4% (w/v) paraformaldehyde solution was added to the medium to give a final concentration of 0.25% (w/v) formaldehyde. Following incubation for 10 min, cells were scraped into 400 μl of ice-cold PBS. They were collected from 100 μl of the cell suspension by centrifugation (500 x *g*, 2 min, 4$^{o}$C) and lysed in 200 μl of Laemmli sample buffer (20 mM Tris-Cl, pH 6.8, 10% (v/v) glycerol, 0.8% (w/v) SDS, 0.1% (w/v) bromophenol blue, 0.72 M 2-mercaptoethanol) to generate an input sample. The cells present in the remaining portion of each suspension were harvested by centrifugation (500 x *g*, 2 min, 4 $^{o}$C), and lysed in 0.5 ml of Buffer A (6 M guanidine hydrochloride, 10 mM Tris, 0.1 M phosphate buffer, pH 8.0, 0.1% (v/v) Triton X-100) supplemented with 6 mM imidazole. The lysate was sonicated, clarified by centrifugation (16,000 x *g*, 3 min, 20 $^{o}$C), and the

resulting solution was added to 50 µl of Ni-CAM® HC resin (Sigma). The resulting suspension was incubated with end-over-end rotation for 3 h at 20°C. Thereafter, the Ni-CAM HC resin was washed sequentially with Buffer A, Buffer B (8 M Urea, 10 mM Tris, 0.1 M phosphate buffer, pH 8.0, 0.1% (v/v) Triton X-100) and Buffer C (8 M Urea, 10 mM Tris, 0.1 M phosphate buffer, pH 6.3, 0.1% (v/v) Triton X-100). Material that remained bound after washing with Buffer C was eluted from the resin and the formaldehyde cross-links reversed by suspension of the resin in 50 µl of Laemmli SDS sample buffer supplemented with 300 mM imidazole, followed by boiling for 15 min. The suspension was centrifuged (16,000 x *g*, 1 min, 20 °C) and the supernatant was collected and referred to as the 'IP' fraction.

*Live-cell Förster resonance transfer (FRET) microscopy*

The FRET efficiency displayed by all Keap1-based FRET reporter molecules was measured using live-cell acceptor photobleaching RET on a DeltaVision Core restoration microscope (Applied Precision, USA) with a 12-bit Coolsnap HQ camera (Roper Scientific, USA) mounted on an Olympus IX71 stand and with a 100x 1.35 NA PlanApo lens. The microscope was temperature controlled at 37°C using a Solent Scientific environmental chamber (Solent Scientific, UK). The light source used was a 300 W Xenon lamp. Images were acquired at a 512 x 512 resolution with a 2 x 2 bin and an exposure time of 0.1 s. The Cerulean channel used a D436/10x Excitation Filter (Chroma) and an ET480/40m Emission Filter (Chroma). The EYFP channel used a D500/20x Excitation Filter (Chroma) and an ET535/30m Emission Filter. The EYFP fluorescence was photobleached using a single 0.5 s bleach event using a 5 mW 532 nm

laser line (Qioptiq, USA) focused to a diffraction limited spot in the centre of the field of view. For each cell analyzed, five pre-laser event images were acquired, followed by twelve post-event images using either the Cerulean channel or the EYFP channel, as appropriate. The mean Cerulean or EYFP intensity in the region of interest around the laser spot at each time-point ($Cerulean_{t=1}$…$Cerulean_{t=17}$; $EYFP_{t=1}$…$EYFP_{t=17}$) was then extracted using SoftWorx software (Applied Precision, USA). To measure the FRET efficiency (FE) in a population of cells under a particular experimental condition, the BLEACH efficiency ($BE = (EYFP_{t=5} - EYFP_{t=6})/EYFP_{t=5}$) was measured first in each of ten cells and averaged ($BE_{average}$). Next, FE ($1/(1 + (BE_{average} \times (Cerulean_{t=5}/(Cerulean_{t=6} - Cerulean_{t=5})))))$ was measured in each of another 40 cells.

*Model construction*

A structure for amino-acids 60-624 of mKeap1 was obtained by homology-modelling using MODELLER Release 9v7 software (Šali and Blundell, 1993) and the following template structures: 1BUO.pdb, 1R29.pdb, 2IHC.pdb, 2NN2.pdb, 2PPI.pdb, 2Q81.pdb, 2VKP.pdb, 2YY9.pdb, 2Z8H.pdb, 3B84.pdb, 3DRZ.pdb, 3E4U.pdb, 3FKC.pdb, (all BTB domain structures) 3HTM.pdb, 3HVE.pdb, 3I3N.pdb (BTB-BACK structures) and 1X2J.pdb (a structure of the mKeap1 Kelch domain). The resulting model was refined using MOLPROBITY (Davis et al., 2004) to flip certain His and Asp residues and to optimize the hydrogen-bonding network. A structure for the Keap1 homodimer was obtained by superimposing a Keap1 monomer upon each of the two BTB domains present in the structure of the BTB homodimer from BCL6 (1R28.pdb). $CRL3^{Keap1}$ and related models were generated using the approach outlined by Orlicky et al. (Orlicky et al., 2003) . Firstly, the Keap1 homodimer was superimposed upon the Skp1 structure in

the Cul1-Rbx1-Skp1-Skp2 structure (1LDK.pdb), and Skp1 and Skp2 were subsequently deleted. Cul1 was used as a proxy for Cul3 and the resulting structure is used to represent $CRL^{Keap1}$. Secondly, Ub~UbcH7 was placed upon this complex as follows; the RING domain of the cCbl-UbcH7 structure (1FBV.pdb) was superimposed upon the RING domain of Rbx1, and cCbl was subsequently deleted. Ub was positioned by superimposing Ub~E2-24 with UbcH7 and subsequently deleting E2-24. Collectively, these manipulations generate a representation of $CRL^{Keap1}$-Ub~UbcH7.

## RESULTS

*Zinc can be sensed by Keap1 through co-ordination chemistry*

We reported previously that $Zn^{2+}$ (and other metal(loids) such as $Cd^{2+}$, $As^{3+}$ and $Se^{4+}$) are sensed by Keap1 through a direct-binding mechanism involving co-ordination by His-225, Cys-226, and Cys-613 of the protein (McMahon et al., 2010) . However, one concern over the definition of this $Zn^{2+}$ sensor was that the dependence of Keap1 on these residues for metal(loid) sensing was not absolute (see for example Fig 4 in (McMahon et al., 2010) ). In fact, when a solution of $ZnCl_2$ is added to culture medium, the His-225/Cys-226/Cys-613 triad is only important for sensing the metal over a relatively narrow concentration range (**Fig 1B**). However, as cell culture medium contains many metal-binding proteins that can 'buffer' free zinc, we postulated that the sharp transition between the ability of Keap1 to sense zinc in a manner dependent on His-225/Cys-226/Cys-613 and in a manner independent of this triad of residues occurs when the buffering capacity of the medium is exceeded, which would in turn lead to an apparent surge in the concentration of free zinc available for uptake into cells by zinc transporters. To test this hypothesis, we pre-chelated zinc with cell-permeable pyrithione, reasoning that this would circumvent both the buffering capacity of the medium and reliance on zinc transporters for uptake of the metal into cells. Indeed, consistent with the notion that culture medium buffers zinc, we found that following treatment with pyrithione much less zinc was required to stabilize ectopic mNrf2-V5 in COS1 cells, and His-225/Cys-226/Cys-613 dependency was observed over a dramatically wider range of concentrations of the metal (**Fig 1B**).

Although the ability of Keap1 lacking residues His-225/Cys-226/Cys-613 to detect $Zn^{2+}$ is significantly impaired, dependency on these three residues is still not absolute, hinting that some redundancy may exist in the identity of amino-acids in Keap1 that bind the metal. Also consistent with the idea of redundancy, was our inability to identify a single additional amino-acid that fulfilled the role of providing a fourth co-ordinating ligand, despite the fact we generated a comprehensive panel of Keap1 expression constructs in which all 25 cysteine and 20 histidine residues were replaced individually. Although three of these mutant proteins were inactive (i.e. Keap1 bearing H96N, C171S, or H311N substitutions), and thus uninformative, none of the remaining mutant proteins were impaired at responding to free $Zn^{2+}$ (data not shown). We therefore propose that Keap1 uses a redundant set of amino-acids to co-ordinate and, thus, detect metal(loid)s; amongst these, His-225, Cys-226, and Cys-613 are of paramount importance, but none are indispensable.

*The $Zn^{2+}$ sensor in Keap1 operates independently of p62*

During the present study, we observed that Keap1 formed aggregates in response to treatment with $Zn^{2+}$ (**Fig 2A**), $Cd^{2+}$ (**Fig 2B**), and, consistent with earlier reports (Lau et al., 2013) , $As^{3+}$ (**Fig 2B**). Aggregation of Keap1 appears to be a direct consequence of engagement of the $Zn^{2+}$ sensor as it was prevented by disabling mutations in Keap1 (**Fig 2A** & **B**). However, the tendency of Keap1 to aggregate is not intrinsic to the action of the $Zn^{2+}$ sensor because the metalloid $Se^{4+}$ is a potent trigger of the sensor (McMahon et al., 2010) but it does not cause aggregation of the BTB-Kelch protein (**Fig 2B**).

Keap1 aggregates that formed upon treatment with free $Zn^{2+}$ became 'decorated' with p62 (**Fig 2C**). To investigate whether p62 might be necessary for sensing zinc, we compared the response of wild-type and *p62*$^{-/-}$ MEF cells to the metal. Nrf2 accumulated in fibroblasts of both *p62*$^{+/+}$ and *p62*$^{-/-}$ fibroblasts (**Fig 2D**) confirming that Keap1 can sense $Zn^{2+}$ independently of the autophagy adaptor protein. The $Zn^{2+}$ sensor and the previously-described non-canonical p62 signalling pathway (Lau et al., 2013) therefore represent distinct mechanisms by which Keap1 may be triggered to alleviate Nrf2 turnover.

How and why Keap1 aggregates in response to triggering of its $Zn^{2+}$ sensor, and the significance of the association between these aggregates and p62 warrants further study. Notably, it has been reported that p62 can promote turnover of Keap1 by recruiting it to autophagosomes (Taguchi et al., 2012) . Although p62 does not appear to play such a role in healthy MEF cells, as indicated by similar levels of the BTB protein in *p62*$^{+/+}$ and *p62*$^{-/-}$ MEFs, treatment with $Zn^{2+}$ generally caused a modest reduction in Keap1 levels and this was dependent on p62 (**Fig 2D**). On this basis, we suggest that p62 might be involved in clearing Keap1 aggregates that are formed upon treatment with metal(loid)s.

*The interaction between Keap1 and Nrf2 persists in stressed cells*

To investigate how triggering of the various sensor systems in Keap1 attenuates Nrf2 ubiquitylation by the $CRL^{Keap1}$ complex, we first explored whether the Keap1-Nrf2 interaction persists in stressed cells. COS1 cells co-expressing EGFP-mKeap1 and mNrf2$^{\Delta 17\text{-}32}$-V5 were treated with chemicals chosen from amongst those tabulated in **Fig**

**1A**; we selected mNrf2$^{\Delta 17\text{-}32}$-V5 for these experiments because it lacks the DLG motif and, therefore, it interacts with Keap1 only through its high-affinity ETGE motif without becoming ubiquitylated (McMahon et al., 2006) . The tagged transcription factor co-immunoprecipitated with EGFP-mKeap1 from lysates prepared from control or treated cells, demonstrating that the interaction between the two proteins was unaffected by stimulation of any of the tested sensors in Keap1 (**Fig 3A**). Moreover, this conclusion holds true for intact cells also, as assessed by *in vivo* cross-linking of the two proteins (**Fig 3B**) and by immunocytochemistry (**Fig 3C**). The latter data are particularly compelling; mNrf2$^{\Delta 17\text{-}32}$-V5 was present exclusively in the nucleus when it was expressed on its own (**Fig 3C,** *top row*), but when co-expressed with EGFP-mKeap1 a portion of the CNC-bZIP transcription factor was retained in the cytoplasm (**Fig 3C**, *second row*). Critically, engagement of mNrf2$^{\Delta 17\text{-}32}$-V5 by EGFP-mKeap1 was not antagonised by Sul, tBHQ, Acro or $Cd^{2+}$ (**Fig 3C**).

The conclusion that the Keap1-Nrf2 interaction occurs constitutively, and is not an artefact of over-expression, can be drawn from our finding that endogenous Nrf2 co-immunoprecipitated with endogenous Keap1, regardless of whether the tested sensors in the BTB protein had been triggered or not (**Fig 4A**). Parallel experiments with *Keap1*$^{-/-}$ fibroblasts confirmed that the presence of Nrf2 in the immuno-precipitates was absolutely dependent upon Keap1 (**Fig 4A**). Also in agreement with the over-expression data was our finding, using highly specific (**Fig 4B**) affinity-purified antibodies, that endogenous mNrf2 is found exclusively in the nucleus of both stressed cells (wild-type fibroblasts treated with Sul) and healthy cells (wild-type fibroblasts treated with vehicle or MG132, the latter of which was used to allow a detectable pool of mNrf2 to accumulate in the

absence of stress) (**Fig 4C**); these findings support the work of Nguyen *et al*. (Nguyen et al., 2005) , who reported Nrf2 to be constitutively nuclear.

Collectively, these data support the previous report (Baird et al., 2013) that the interaction *in vivo* between Keap1 and Nrf2 is not antagonized by xenobiotics that target the Keap1/Nrf2 axis.

*The $CRL^{Keap1}$ complex persists in stressed cells*

Although our results indicate that Keap1 constitutively engages Nrf2, it has also been suggested that stress causes disassembly of $CRL^{Keap1}$ itself – either by dissociation (Eggler et al., 2009; Rachakonda et al., 2008; Zhang et al., 2004) or by degradation of Keap1 (Hong et al., 2005; Zhang et al., 2005) . The hypothesis that stressors stimulate degradation of Keap1 is not supported by our finding that the endogenous levels of Keap1 in untreated fibroblasts are largely unchanged in fibroblasts challenged with Sul, tBHQ, Acro or $Cd^{2+}$ (**Fig 4A** & **Fig 5A**), with the Keap1 protein having a half-life of approximately 200 min in control cells (**Fig 5B**). Moreover, we also found that levels of ectopic mKeap1 were unaffected by stress (e.g. **Fig 5C**) as was their propensity to self-associate (**Fig 5C** & **D**). These data strongly suggest that dimeric Keap1 is constantly available to associate with the Cul3-Rbx1 holoenzyme.

At first glance, the idea that triggering the stress sensors in Keap1 might cause it to dissociate from CRL is an appealing one, at least for the NO sensor, as it resides in the same BTB domain that interacts with Cul3. Our molecular modelling however indicated that the NO sensor is unlikely to be present at the interface between Keap1 and Cul3 (**Fig S1**). Moreover, we found that the two proteins interact constitutively, as ECFP-mCul3

co-immunoprecipitated with mKeap1-V5-his from COS1 lysates under all conditions, including those that trigger the NO sensor (**Fig 6A**). The interaction between the two proteins persists also in intact cells, as demonstrated by *in vivo* cross-linking experiments with mKeap1-V5-his and ECFP-mCul3 (**Fig 6B**). We validated this interpretation by confirming that the cross-linking of mKeap1-V5-his with ECFP-mCul3 required their direct association *in vivo*. Thus, when Ser-50 and Phe-52 of mCul3, which are essential for the interaction between Cul3 and BTB proteins (Furukawa et al., 2003) , were replaced with Ala residues, the resulting mutant ECFP-mCul3$^{SF\text{-}AA}$ protein retained the ability of the wild-type protein to cross-link to Rbx1 (**Fig S2A**) – but not to the his-tagged adaptor protein (**Fig S2B**).

Although the interaction between Keap1 and Cul3 occurs constitutively, we noted that the affinity of the two proteins for each other was diminished in the presence of chemicals that trigger the NO sensor (**Fig 6A**). Attenuation of this interaction clearly required stimulation of the NO sensor as it was not observed when Keap1 contained the C151S amino-acid substitution (which disables the sensor) (**Fig 6C**).

Finally, we attempted to verify that stimulating the stress sensors of endogenous mKeap1 does not prevent it from interacting with endogenous mCul3. Unfortunately, this proved technically impossible as we were unable to detect mCul3 in mKeap1 immuno-precipitates, even when they were prepared from unstressed fibroblasts (data not shown).

*Triggering of the $Zn^{2+}$ Sensor causes a conformational switch in Keap1*

The data described above suggest that Nrf2 continues to interact with CRL$^{Keap1}$ regardless of whether stress sensors in Keap1 have been triggered. We therefore considered the

possibility that one-or-more of the sensors might stabilize Nrf2 by operating as conformational switches (McMahon et al., 2006; Kit I. Tong et al., 2006) . We examined this hypothesis using a genetically-encoded intramolecular FRET reporter molecule that was designed to register changes in the overall structure of Keap1. The Keap1-based FRET reporter comprises a monomeric variant of the fluorescent Cerulean protein (blue) fused to the *N*-terminus of mKeap1, with the Kelch-repeat domain of the adaptor protein replaced by a monomeric variant of EYFP (yellow). We found the resulting fusion protein, mKeap1FRET, to be functional insofar as it associated with mKeap1 and mCul3 (**Fig S3A-B**). In control COS1 cells, mKeap1FRET displayed a FRET efficiency of approximately 25% (**Fig S3C**). The measured signal truly represents FRET because it was almost completely ablated (**Fig S3C**) by two amino-acid substitutions (S65T and G67A) that preclude formation of the fluorophore structure in EYFP (Wielgus-Kutrowska et al., 2007) . Moreover, the FRET signal was not recovered by co-expressing EYFP as a separate polypeptide (**Fig S3C**).

The extent of FRET within the reporter was unchanged upon exposure of cells to two chemicals, Sul (**Fig 7A**) and NO (data not shown) that trigger the NO sensor. Moreover, the alkenal 4HNE, which acts, at least in part, by *S*-alkylation of Cys-288 (McMahon et al., 2010; Saito et al., 2016), also failed to elicit a change in the FRET signal (**Fig 7B**). Treatment with the more reactive alkenal acrolein stimulated a significant change in FRET efficiency; although this chemical covalently modifies Cys-151 and Cys-288, the implied conformational change did not require *S*-alkylation of either residue as indicated by the use of mutated mKeap1FRET reporters bearing Ser residues in place of these Cys residues (**Fig S3D** & **E**). By contrast, $Zn^{2+}$, its ionic mimic

491 $Cd^{2+}$, and also $As^{3+}$, increased the FRET efficiency of the reporter molecule (**Fig 7C-E**).
492 Crucially, this change was prevented in all instances by substituting two amino-acids
493 (His-225 and Cys-226) that are required for the $Zn^{2+}$ sensor. We also noticed that the
494 magnitude of the conformation shift elicited by stimulating the $Zn^{2+}$ sensor
495 ($Zn^{2+}$>$Cd^{2+}$>$As^{3+}$>$Se^{4+}$) was inversely correlated with the size of the 'trigger' chemical.
496 Indeed, $Se^{4+}$ did not drive any noticeable change in FRET efficiency of the Keap1-based
497 reporter (**Fig 7F**).
498

## DISCUSSION

*Operation of the Zinc sensor*.

In our original identification of the $Zn^{2+}$ sensor in murine Keap1 (McMahon et al., 2010) , we suggested it comprises minimally amino acids His-225, Cys-226, and Cys-613. At that time, we felt it unlikely these three residues fully describe the sensor because from chemical considerations, and characterization of Zn-binding proteins, it seemed likely that $Zn^{2+}$ would be co-ordinated by a fourth amino acid side-chain. Following individual site-directed mutagenesis of all Cys and His residues in Keap1, we have been unable to identify a single amino acid within the BTB–Kelch-repeat protein that uniquely fulfils the putative role of providing a fourth co-ordinating interaction with $Zn^{2+}$ (data not shown), suggesting that instead multiple redundant amino acids may do so. Indeed, not even the three $Zn^{2+}$ co-ordinating ligands are absolutely required; specifically, in the absence of His-225, Cys-226 and Cys-613, $Zn^{2+}$ can still be sensed weakly by Keap1 (**Fig 1B** & **C**). Taking all available evidence into account, we now prefer the hypothesis that multiple amino acids within Keap1 may co-ordinate metal ions.

The notion that multiple amino acids in Keap1 bind metal(loid)s may also help explain the tendency of Keap1 to form aggregates. It was previously reported that arsenite causes aggregation of Keap1 (Lau et al., 2013) . Our data suggest such aggregation may be a common consequence of triggering the $Zn^{2+}$ sensor as both $Zn^{2+}$ and $Cd^{2+}$ also cause aggregation of the BTB–Kelch-repeat protein, but only when the $Zn^{2+}$ sensor is intact. Interestingly, aggregation is a feature of disordered proteins. Thus, if multiple amino acid side-chains in Keap1 can co-ordinate zinc, then this might give rise to a pseudo-disordered population of Keap1 molecules with different conformations,

522 some of which may be prone to aggregate. Supporting this hypothesis, the only trigger of
523 the $Zn^{2+}$ sensor that does not cause aggregation of Keap1 is selenite and, significantly,
524 this metal(loid) showed absolute dependence on His-225, Cys-226, and Cys-613 in our
525 previous study (McMahon et al., 2010) .

526 The contribution of p62 to the operation of the Keap1 $Zn^{2+}$ sensor requires further
527 investigation. This sensor does not require the presence of the p62 autophagy adaptor as
528 we have found it can be triggered in p62-null cells. Yet, p62 is recruited to Keap1
529 aggregates formed upon engagement of the $Zn^{2+}$ sensor. The consequences of recruitment
530 of p62 to these aggregates remain unclear at present. It might be relevant that the affinity
531 of Keap1 for $Zn^{2+}$ (Dinkova-Kostova et al., 2005) is such that the active *apo*-form of
532 the adaptor protein might be expected to be only slowly regenerated once the cellular
533 stressor that elicited the surge in intracellular free $Zn^{2+}$ has dissipated. It is tempting
534 therefore to suggest that p62 might target metallated Keap1 to autophagosomes to remove
535 the inactive form of the adaptor and accelerate the re-setting of the Keap1-based
536 monitoring system to its homeostatic set-point. This concept is supported by earlier work
537 showing that iron-binding proteins, such as ferritin or transferrin, are trafficked to
538 lysosomes or endosomes for degradation or re-generation of the free metal and the *apo*-
539 protein (Asano et al., 2011; Eckenroth et al., 2011) .

540

541 *Evidence that conformational changes in Keap1 control Nrf2 stability*.

542 We have found that Nrf2 continues to be recruited to $CRL^{Keap1}$ in stressed cells;
543 perplexingly, whilst the transcription factor binds Keap1, it simply fails to become
544 ubiquitylated in stressed cells. This is consistent with an earlier suggestion from us

(McMahon et al., 2010, 2006) and others (Ogura et al., 2010; Kit I. Tong et al., 2006) that Nrf2 might evade ubiquitylation and accumulate as a consequence of stress-triggered conformational switches in Keap1 that mis-align the transcription factor with the Ub~E2 protein upon the E3 complex. Our finding using a genetically-encoded FRET reporter that Keap1 changes conformation in living cells exposed to agents that stimulate the $Zn^{2+}$ sensor provides experimental support for this hypothesis. Notably, this switch does not drive a monolithic change in Keap1 structure. Instead, it seems that Keap1 is flexible and can adopt various conformations depending on the characteristics (such as size, hydrophobicity and charge) of the xenobiotics that interact with it (**Figure 7C-F**). In fact, $Se^{4+}$ triggers the $Zn^{2+}$ sensor but does not cause a measurable change in FRET using our conformation reporter construct. One important caveat to this interpretation is that our reporter construct lacks Cys-613 and the failure of selenite to trigger a change in FRET efficiency may simply be due to it being more dependent on Cys-613 for binding to Keap1 than are the other meta(loid)s.

Molecular-modeling (**Fig S1**) and cryo-EM studies (Ogura et al., 2010) of Keap1 provide important clues as to the structural consequences of stimulating the $Zn^{2+}$ sensor, and how this might hinder the ubiquitylation of Nrf2. The two BTB domains in the two Keap1 subunits within $CRL^{Keap1}$ are constrained by self-association (McMahon et al., 2006) , and they therefore act as pivot points around which the Kelch-repeat domain 'loads' might be moved by the BACK (i.e. BTB and C-terminal Kelch (Stogios and Privé, 2004)) domains, which act as 'armatures'. Crucially, the $Zn^{2+}$ sensor involves residues that reside in the BACK domain. It therefore seems likely that $Zn^{2+}$ binding to Keap1 distorts the structure of the BACK domain in the adaptor protein and, in so doing,

alters the pre-existing spatial relationship between the two Kelch-repeat domains within the $CRL^{Keap1}$ complex (**Fig S1**). Moreover, it is reasonable to conclude, on statistical grounds alone, that the resulting displacement of the Kelch-repeat domains is likely to stabilize Nrf2. This is because the mechanics of the ubiquitylation reaction are such that only a small number of all conceivable positions of the two domains, relative to each other, are compatible with Nrf2 turnover. For example, as the two Keap1-binding sites in Nrf2 are found at opposite ends of a long (54 Å) α-helix, only a limited number of arrangements of the Kelch-repeat domains will be compatible with the 54 Å spacing required to allow the two-site interaction that is a prerequisite for Nrf2 ubiquitylation. It seems likely that other geometric constraints will become apparent as our understanding of the mechanism of ubiquitylation deepens. Of course, detailed biophysical studies will ultimately be necessary to clarify the finer details of the molecular processes outlined above.

*How do the NO sensor and the alkenal sensor regulate Nrf2 turnover?*

Further research is required to answer the question of how NO and alkenals block ubiquitylation of Nrf2 by triggering their cognate sensors in Keap1. For, unlike the $Zn^{2+}$ sensor, our FRET experiments do not support the idea that stimulation of the NO (Cys-151) sensor or the alkenal (Cys-288) sensor drive large, global conformation shifts in Keap1. However, we must add the caveat that the engineered reporter we have employed is an imperfect model of Keap1. Consequently, these findings may simply reflect a failure of the reporter to sense and/or respond appropriately to signals that are recognized by these two stress sensors. Nevertheless, the most plausible interpretation of these data

591 is that triggering the Cys-151 and Cys-288 sensors elicit more subtle conformational
592 changes than does triggering of the $Zn^{2+}$ sensor. The modelled structure of the NO sensor,
593 is in fact compatible with this interpretation (McMahon et al., 2010) ; such changes
594 might account also for the marginal reduction in affinity of Keap1 for Cul3 that we
595 observed when this sensor was stimulated (**Fig 6A** & **C**).
596
597 *Spatial organisation of the Keap1-Nrf2 complex*
598 We have found that Nrf2 is a steady-state nuclear protein rather than a cytoplasmic one
599 and, thus, it resides in a separate subcellular compartment to Keap1 (Watai et al.,
600 2007) . This observation raises the question of how Keap1 can determine directly the
601 fate of Nrf2. One explanation for this may lie with the reported ability of Nrf2 to shuttle
602 between the nucleus and the cytoplasm (Li et al., 2005) . As long as this nucleo-
603 cytoplasmic shuttling is not the rate-limiting step in the overall process leading to
604 ubiquitylation, then the actual distribution of Nrf2 at steady-state becomes irrelevant. It is
605 therefore possible that Nrf2 routinely traffics in-and-out of the nucleus, continuously
606 engaging and disengaging from Keap1.
607 Another explanation is that Keap1 acts as a type of gatekeeper that 'intercepts'
608 and turns-over *de novo* translated Nrf2 as it translocates from the cytoplasm into the
609 nucleus, and that once in the nucleus the stability of Nrf2 is controlled by the β-
610 transducin repeat-containing protein (β-TrCP) and glycogen synthase kinase-3 (GSK-3)
611 axis (Chowdhry et al., 2013; Rada et al., 2011) . In this case, Nrf2 within the nucleus is
612 first phosphorylated by GSK-3 at a DSGIS motif in its Neh6 domain before it is
613 ubiquitylated by the Skp1–Cul1–F-box (SCF) ubiquitin ligase designated $SCF^{\beta\text{-TrCP}}$; thus

GSK-3 creates a DSGIS-containing phosphodegron in the Neh6 domain of Nrf2 that is recognised by $SCF^{\beta\text{-}TrCP}$. In this scenario, Keap1 controls nuclear entry of Nrf2, whereas GSK-3 in conjunction with β-TrCP controls the stability of Nrf2 in the nucleus. The relative importance of $CRL^{Keap1}$ and $SCF^{\beta\text{-}TrCP}$ in regulating the activity of Nrf2 is not clear but may be tissue specific, dependent on the subcellular location of GSK-3 isoenzymes, and influenced by nutrient status. In this regard, growth factor signalling that inhibits the activity of GSK-3 (via the actions of protein kinase B (PKB)/Akt) likely induces Nrf2-target gene expression in a Keap1-independent manner (for a review, see (Hayes et al., 2016) ).

*Concluding comments*.

On the basis of the data presented herein along with that in the literature, we suggest the model depicted in **Figure S4** to account for the operation of the Keap1-Nrf2 system in health and disease. Moving beyond Keap1-Nrf2 biochemistry, we suspect that conformational switches, analogous to the $Zn^{2+}$ sensor, will be commonly employed by various classes of CRL to control the half-life of their substrates. This prediction is based on the fact that structural plasticity is not a peculiarity of Keap1; earlier work suggested that a number of meprin and TRAF-C homology (MATH)-BTB proteins also contain a flexible linker between their substrate recognition (i.e. MATH) and BTB domains (Zhuang et al., 2009) . In fact, any CRL that contains a dimeric substrate adaptor, and which recruits substrates via a two-site docking mechanism, is a likely candidate to contain such switches.

**Acknowledgements**:

We thank Cancer Research UK (grants C4909/A5942 and C4909/A9990) and the Medical Research Council (grant MR/N009851/1) for funding our work. We are grateful to Professor Masaaki Komatsu (University of Niigata, Japan) for providing *p62*$^{-/-}$ and *p62*$^{+/+}$ MEF cells, and Professor Masayuki Yamamoto (Tohoku University, Japan) for providing *Keap1*$^{-/-}$ MEF cells.

## REFERENCES


Abiria, S.A., Krapivinsky, G., Sah, R., Santa-cruz, A.G., Chaudhuri, D., Zhang, J., 2017. TRPM7 senses oxidative stress to release Zn 2 + from unique intracellular vesicles 7. https://doi.org/10.1073/pnas.1707380114

Asano, T., Komatsu, M., Yamaguchi-iwai, Y., Ishikawa, F., Iwai, K., Corporation, T., Project, P.M., Biology, C., Medical, T., Group, M., 2011. Distinct mechanisms of ferritin delivery to lysosomes in iron- depleted and iron-replete cells. https://doi.org/10.1128/MCB.01437-10

Baird, L., Llères, D., Swift, S., Dinkova-Kostova, A.T., 2013. Regulatory flexibility in the Nrf2-mediated stress response is conferred by conformational cycling of the Keap1-Nrf2 protein complex. Proc. Natl. Acad. Sci. 110, 15259 LP-15264.

Canning, P., Cooper, C.D.O., Krojer, T., Murray, J.W., Pike, A.C.W., Chaikuad, A., Keates, T., Thangaratnarajah, C., Hojzan, V., Marsden, B.D., 2013. Structural basis for Cul3 assembly with the BTB-Kelch family of E3 ubiquitin ligases. https://doi.org/10.1074/jbc.M112.437996

Canning, P., Sorrell, F.J., Bullock, A.N., 2015. Structural basis of Keap1 interactions with Nrf2. Free Radic. Biol. Med. 88, 101–107. https://doi.org/https://doi.org/10.1016/j.freeradbiomed.2015.05.034

Chen, P.-H., Smith, T.J., Wu, J., Siesser, P.F., Bisnett, B.J., Khan, F., Hogue, M., Soderblom, E., Tang, F., Marks, J.R., Major, M.B., Swarts, B.M., Boyce, M., Chi, J.-T., 2017. Glycosylation of KEAP1 links nutrient sensing to redox stress signaling. EMBO J. 36, 2233–2250. https://doi.org/10.15252/embj.201696113

Chowdhry, S., Zhang, Y., McMahon, M., Sutherland, C., Cuadrado, A., Hayes, J.D., 2013. Nrf2 is controlled by two distinct beta-TrCP recognition motifs in its Neh6 domain, one of which can be modulated by GSK-3 activity. Oncogene. https://doi.org/10.1038/onc.2012.388

Dargel, R., 1992. Lipid peroxidation — a common pathogenetic mechanism? Exp. Toxicol. Pathol. 44, 169–181. https://doi.org/https://doi.org/10.1016/S0940-2993(11)80202-2

Davis, I.W., Murray, L.W., Richardson, J.S., Richardson, D.C., 2004. MolProbity: structure validation and all-atom contact analysis for nucleic acids and their complexes. Nucleic Acids Res. 32, W615–W619.

Dinkova-Kostova, A.T., Holtzclaw, W.D., Cole, R.N., Itoh, K., Wakabayashi, N., Katoh, Y., Yamamoto, M., Talalay, P., 2002. Direct evidence that sulfhydryl groups of Keap1 are the sensors regulating induction of phase 2 enzymes that protect against carcinogens and oxidants. Proc. Natl. Acad. Sci. 99, 11908 LP-11913.

Dinkova-Kostova, A.T., Holtzclaw, W.D., Wakabayashi, N., 2005. Keap1, the Sensor for Electrophiles and Oxidants that Regulates the Phase 2 Response, Is a Zinc Metalloprotein. Biochemistry 44, 6889–6899. https://doi.org/10.1021/bi047434h

Eckenroth, B.E., Steere, A.N., Chasteen, N.D., Everse, S.J., Mason, A.B., 2011. How the binding of human transferrin primes the transferrin receptor potentiating iron release at endosomal pH. Proc. Natl. Acad. Sci. 108, 13089 LP-13094.

Eggler, A.L., Small, E., Hannink, M., Mesecar, A.D., 2009. Cul3-mediated Nrf2 ubiquitination and antioxidant response element (ARE) activation are dependent on the partial molar volume at position 151 of Keap1. Biochem. J. 422, 171 LP-180.

Eide, D.J., 2006. Zinc transporters and the cellular trafficking of zinc. Biochim. Biophys. Acta - Mol. Cell Res. 1763, 711–722. https://doi.org/https://doi.org/10.1016/j.bbamcr.2006.03.005

Fourquet, S., Guerois, R., Biard, D., Toledano, M.B., 2010. Activation of NRF2 by Nitrosative Agents and H2O2 Involves KEAP1 Disulfide Formation. J. Biol. Chem. 285, 8463–8471.

Furukawa, M., He, Y.J., Borchers, C., Xiong, Y., 2003. Targeting of protein ubiquitination by BTB–Cullin 3–Roc1 ubiquitin ligases. Nat. Cell Biol. 5, 1001.

Gasch, A.P., 2007. Comparative genomics of the environmental stress response in ascomycete fungi. Yeast 24, 961–976. https://doi.org/10.1002/yea.1512

Hayes, J.D., Dinkova-kostova, A.T., 2014. The Nrf2 regulatory network provides an interface between redox and intermediary metabolism. Trends Biochem. Sci. 39, 199–218. https://doi.org/10.1016/j.tibs.2014.02.002

Hayes, J.D., Ebisine, K., Sharma, R.S., Chowdhry, S., Dinkova-Kostova, A.T., Sutherland, C., 2016. Regulation of the CNC-bZIP transcription factor Nrf2 by Keap1 and the axis between GSK-3 and β-TrCP. Curr. Opin. Toxicol. 1, 92–103. https://doi.org/https://doi.org/10.1016/j.cotox.2016.10.003

Hayes, J.D., McMahon, M., 2009. NRF2 and KEAP1 mutations: permanent activation of an adaptive response in cancer. Trends Biochem. Sci. https://doi.org/10.1016/j.tibs.2008.12.008

Hecker, M., Pané-Farré, J., Uwe, V., 2007. SigB-Dependent General Stress Response in Bacillus subtilis and Related Gram-Positive Bacteria. Annu. Rev. Microbiol. 61, 215–236. https://doi.org/10.1146/annurev.micro.61.080706.093445

Hengge-Aronis, R., 1999. Interplay of global regulators and cell physiology in the general stress response of Escherichia coli. Curr. Opin. Microbiol. 2, 148–152. https://doi.org/https://doi.org/10.1016/S1369-5274(99)80026-5

Holland, R., Fishbein, J.C., 2010. Chemistry of the Cysteine Sensors in Kelch-Like ECH-Associated Protein 1. Antioxid. Redox Signal. 13, 1749–1761. https://doi.org/10.1089/ars.2010.3273

Hong, F., Sekhar, K.R., Freeman, M.L., Liebler, D.C., 2005. Specific Patterns of Electrophile Adduction Trigger Keap1 Ubiquitination and Nrf2 Activation. J. Biol. Chem. 280, 31768–31775. https://doi.org/10.1074/jbc.M503346200

Hourihan, J.M., Kenna, J.G., Hayes, J.D., 2012. The Gasotransmitter Hydrogen Sulfide Induces Nrf2-Target Genes by Inactivating the Keap1 Ubiquitin Ligase Substrate Adaptor Through Formation of a Disulfide Bond Between Cys-226 and Cys-613. Antioxid. Redox Signal. 19, 465–481. https://doi.org/10.1089/ars.2012.4944

Ichimura, Y., Waguri, S., Sou, Y., Kageyama, S., Hasegawa, J., Ishimura, R., Saito, T., Yang, Y., Kouno, T., Fukutomi, T., Hoshii, T., Hirao, A., Takagi, K., Mizushima, T., Motohashi, H., Lee, M., Yoshimori, T., Tanaka, K., 2013. Article Phosphorylation of p62 Activates the Keap1-Nrf2 Pathway during Selective Autophagy. Mol. Cell 51, 618–631. https://doi.org/10.1016/j.molcel.2013.08.003

Itoh, K., Chiba, T., Takahashi, S., Ishii, T., Igarashi, K., Katoh, Y., Oyake, T., Hayashi, N., Satoh, K., Hatayama, I., Yamamoto, M., Nabeshima, Y., 1997. An Nrf2/Small Maf Heterodimer Mediates the Induction of Phase II Detoxifying Enzyme Genes through Antioxidant Response Elements. Biochem. Biophys. Res. Commun. 236, 313–322. https://doi.org/https://doi.org/10.1006/bbrc.1997.6943

Itoh, K., Wakabayashi, N., Katoh, Y., Ishii, T., Igarashi, K., Engel, J.D., Yamamoto, M., 1999. Keap1 represses nuclear activation of antioxidant responsive elements by Nrf2 through binding to the amino-terminal Neh2 domain. Genes Dev. 13, 76–86.

Jain, A., Lamark, T., Sjottem, E., Larsen, K.B., Awuh, J.A., Overvatn, A., McMahon, M., Hayes, J.D., Johansen, T., 2010. p62/SQSTM1 Is a Target Gene for Transcription Factor NRF2 and Creates a Positive Feedback Loop by Inducing Antioxidant Response Element-driven Gene Transcription. J. Biol. Chem. https://doi.org/10.1074/jbc.M110.118976

744 Kamura, T., Koepp, D.M., Conrad, M.N., Skowyra, D., Moreland, R.J., Iliopoulos, O.,
745 Lane, W.S., Kaelin, W.G., Elledge, S.J., Conaway, R.C., Harper, J.W., Conaway,
746 J.W., 1999. Rbx1, a Component of the VHL Tumor Suppressor Complex and SCF
747 Ubiquitin Ligase. Science (80-. ). 284, 657 LP-661.

748 Katsuragi, Y., Ichimura, Y., Komatsu, M., 2016. ScienceDirect. Curr. Opin. Toxicol. 1,
749 54–61. https://doi.org/10.1016/j.cotox.2016.09.005

750 Kensler, T.W., Wakabayashi, N., Biswal, S., 2007. Cell Survival Responses to
751 Environmental Stresses Via the Keap1-Nrf2-ARE Pathway. Annu. Rev. Pharmacol.
752 Toxicol. 47, 89–116. https://doi.org/10.1146/annurev.pharmtox.46.120604.141046

753 Kitano, H., 2004. Biological robustness. Nat. Rev. Genet. 5, 826.

754 Kültz, D., 2004. MOLECULAR AND EVOLUTIONARY BASIS OF THE CELLULAR
755 STRESS RESPONSE. Annu. Rev. Physiol. 67, 225–257.
756 https://doi.org/10.1146/annurev.physiol.67.040403.103635

757 Lau, A., Zheng, Y., Tao, S., Wang, H., Whitman, S.A., White, E., Zhang, D., 2013.
758 Arsenic Inhibits Autophagic Flux , Activating the Nrf2-Keap1 Pathway in a p62-
759 Dependent Manner 33, 2436–2446. https://doi.org/10.1128/MCB.01748-12

760 Li, W., Jain, M.R., Chen, C., Yue, X., Hebbar, V., Zhou, R., Kong, A.-N.T., 2005. Nrf2
761 Possesses a Redox-insensitive Nuclear Export Signal Overlapping with the Leucine
762 Zipper Motif. J. Biol. Chem. 280, 28430–28438.

763 McMahon, M., Itoh, K., Yamamoto, M., Hayes, J.D., 2003. Keap1-dependent
764 proteasomal degradation of transcription factor Nrf2 contributes to the negative
765 regulation of antioxidant response element-driven gene expression. J. Biol. Chem.
766 https://doi.org/10.1074/jbc.M300931200

767 McMahon, M., Lamont, D.J., Beattie, K.A., Hayes, J.D., 2010. Keap1 perceives stress via
768 three sensors for the endogenous signaling molecules nitric oxide, zinc, and
769 alkenals. Proc. Natl. Acad. Sci. U. S. A. https://doi.org/10.1073/pnas.1007387107

770 McMahon, M., Thomas, N., Itoh, K., Yamamoto, M., Hayes, J.D., 2006. Dimerization of
771 substrate adaptors can facilitate cullin-mediated ubiquitylation of proteins by a
772 “Tethering” mechanism - A two-site interaction model for the Nrf2-Keap1 complex.
773 J. Biol. Chem. https://doi.org/10.1074/jbc.M601119200

774 Mills, E.L., Ryan, D.G., Prag, H.A., Dikovskaya, D., Menon, D., Zaslona, Z.,
775 Jedrychowski, M.P., Costa, A.S.H., Higgins, M., Hams, E., Szpyt, J., Runtsch, M.C.,
776 King, M.S., McGouran, J.F., Fischer, R., Kessler, B.M., McGettrick, A.F., Hughes,
777 M.M., Carroll, R.G., Booty, L.M., Knatko, E. V, Meakin, P.J., Ashford, M.L.J.,
778 Modis, L.K., Brunori, G., Sévin, D.C., Fallon, P.G., Caldwell, S.T., Kunji, E.R.S.,

Chouchani, E.T., Frezza, C., Dinkova-Kostova, A.T., Hartley, R.C., Murphy, M.P., O'Neill, L.A., 2018. Itaconate is an anti-inflammatory metabolite that activates Nrf2 via alkylation of KEAP1. Nature 556, 113.

Nguyen, T., Sherratt, P.J., Nioi, P., Yang, C.S., Pickett, C.B., 2005. Nrf2 Controls Constitutive and Inducible Expression of ARE-driven Genes through a Dynamic Pathway Involving Nucleocytoplasmic Shuttling by Keap1. J. Biol. Chem. 280, 32485–32492. https://doi.org/10.1074/jbc.M503074200

Ogura, T., Tong, K.I., Mio, K., Maruyama, Y., Kurokawa, H., Sato, C., Yamamoto, M., 2010. Keap1 is a forked-stem dimer structure with two large spheres enclosing the intervening, double glycine repeat, and C-terminal domains. Proc. Natl. Acad. Sci. 107, 2842 LP-2847.

Orlicky, S., Tang, X., Willems, A., Tyers, M., Sicheri, F., 2003. Structural Basis for Phosphodependent Substrate Selection and Orientation by the SCF Cdc4 Ubiquitin Ligase 112, 243–256.

Rachakonda, G., Xiong, Y., Sekhar, K.R., Stamer, S.L., Liebler, D.C., Freeman, M.L., 2008. Covalent Modification at Cys151 Dissociates the Electrophile Sensor Keap1 from the Ubiquitin Ligase CUL3. Chem. Res. Toxicol. 21, 705–710. https://doi.org/10.1021/tx700302s

Rada, P., Rojo, A.I., Chowdhry, S., McMahon, M., Hayes, J.D., Cuadrado, A., 2011. SCF/beta-TrCP Promotes Glycogen Synthase Kinase 3-Dependent Degradation of the Nrf2 Transcription Factor in a Keap1-Independent Manner. Mol. Cell. Biol. https://doi.org/10.1128/MCB.01204-10

Saito, R., Suzuki, T., Hiramoto, K., Asami, S., Naganuma, E., Suda, H., Iso, T., Yamamoto, H., Morita, M., Baird, L., Furusawa, Y., Negishi, T., Ichinose, M., Yamamoto, M., 2016. Characterizations of Three Major Cysteine Sensors of Keap1 in Stress 36, 271–284. https://doi.org/10.1128/MCB.00868-15.Address

Šali, A., Blundell, T.L., 1993. Comparative Protein Modelling by Satisfaction of Spatial Restraints. J. Mol. Biol. 234, 779–815. https://doi.org/https://doi.org/10.1006/jmbi.1993.1626

Stogios, P.J., Privé, G.G., 2004. The BACK domain in BTB-kelch proteins. Trends Biochem. Sci. 29, 634–637. https://doi.org/10.1016/j.tibs.2004.10.003

Sykiotis, G.P., Bohmann, D., 2010. Stress-Activated Cap'n'collar Transcription Factors in Aging and Human Disease. Sci. Signal. 3, re3 LP-re3.

812 Taguchi, K., Fujikawa, N., Komatsu, M., Ishii, T., Unno, M., Akaike, T., 2012. Keap1
813 degradation by autophagy for the maintenance of redox homeostasis.
814 https://doi.org/10.1073/pnas.1121572109

815 Tong, K.I., Akira, K., Fumiki, K., Masayuki, Y., 2006. Two-site substrate recognition
816 model for the Keap1-Nrf2 system: a hinge and latch mechanism. Biol. Chem.
817 https://doi.org/10.1515/BC.2006.164

818 Tong, K.I., Katoh, Y., Kusunoki, H., Itoh, K., Tanaka, T., Yamamoto, M., 2006. Keap1
819 Recruits Neh2 through Binding to ETGE and DLG Motifs: Characterization of the
820 Two-Site Molecular Recognition Model. Mol. Cell. Biol. 26, 2887 LP-2900.

821 Watai, Y., Kobayashi, A., Nagase, H., Mizukami, M., McEvoy, J., Singer, J.D., Itoh, K.,
822 Yamamoto, M., 2007. Subcellular localization and cytoplasmic complex status of
823 endogenous Keap1. Genes to Cells 12, 1163–1178. https://doi.org/10.1111/j.1365-
824 2443.2007.01118.x

825 Wielgus-Kutrowska, B., Narczyk, M., Buszko, A., Bzowska, A., Clark, P.L., 2007.
826 Folding and unfolding of a non-fluorescent mutant of green fluorescent protein. J.
827 Phys. Condens. Matter 19, 285223.

828 Yamamoto, M., Kensler, T.W., Motohashi, H., 2018. The KEAP1-NRF2 System: a
829 Thiol-Based Sensor-Effector Apparatus for Maintaining Redox Homeostasis.
830 Physiol. Rev. 98, 1169–1203. https://doi.org/10.1152/physrev.00023.2017

831 Zhang, D.D., Hannink, M., 2003. Distinct Cysteine Residues in Keap1 Are Required for
832 Keap1-Dependent Ubiquitination of Nrf2 and for Stabilization of Nrf2 by
833 Chemopreventive Agents and Oxidative Stress. Mol. Cell. Biol. 23, 8137 LP-8151.

834 Zhang, D.D., Lo, S.-C., Cross, J. V, Templeton, D.J., Hannink, M., 2004. Keap1 Is a
835 Redox-Regulated Substrate Adaptor Protein for a Cul3-Dependent Ubiquitin Ligase
836 Complex. Mol. Cell. Biol. 24, 10941 LP-10953.

837 Zhang, D.D., Lo, S.-C., Sun, Z., Habib, G.M., Lieberman, M.W., Hannink, M., 2005.
838 Ubiquitination of Keap1, a BTB-Kelch Substrate Adaptor Protein for Cul3, Targets
839 Keap1 for Degradation by a Proteasome-independent Pathway. J. Biol. Chem. 280,
840 30091–30099. https://doi.org/10.1074/jbc.M501279200

841 Zhuang, M., Calabrese, M.F., Liu, J., Waddell, M.B., Nourse, A., Hammel, M., Miller,
842 D.J., Walden, H., Duda, D.M., Seyedin, S.N., Hoggard, T., Harper, J.W., White, K.P.,
843 Schulman, B.A., 2009. Structures of SPOP-Substrate Complexes: Insights into Molecular
844 Architectures of BTB-Cul3 Ubiquitin Ligases. Mol. Cell 36, 39–50.
845 https://doi.org/10.1016/j.molcel.2009.09.022
846

## FIGURE LEGENDS

**Figure 1. Keap1 senses $Zn^{2+}$ over a wide concentration range in a His-225, Cys-226, and Cys-613-dependent manner.**

**A**, Table listing chemicals employed in the present study (including NO, tBHQ, Sul and Acro), along with the sensors in Keap1 that they trigger. All environmental cues recognized directly by Keap1 are classified into three tiers on the basis of perceived importance (McMahon et al., 2010) . Of principle significance are endogenous 'danger' signals that are intrinsic to the cell. Of secondary importance are environmental toxins that, while extrinsic to the cell, are sufficiently common that they can reasonably be expected to be encountered frequently. Finally, possibly of less significance, are those compounds that are unlikely to be encountered but which trigger Keap1 purely by chance and/or molecular mimicry of more physiologically-relevant signals. **B**, Ectopic mNrf2-V5 was co-expressed in COS1 cells with either wild-type mKeap1 (w) or a mutant form of mKeap1 (m) that lacks His-225, Cys-226, and Cys-613 ($mKeap1^{H225Y,C226S,C613S}$). Post-transfection (24 h), single dishes of cells were exposed to increasing concentrations of either $Zn^{2+}$-pyrithione complex (ZnPy), or free $Zn^{2+}$ ($ZnCl_2$). The amount of mNrf2-V5 present in each culture after 2 h of treatment was quantified by immunoblot. The starting concentration (X) for $Zn^{2+}$-Py complex was 1 μmol/l and it was 112.5 μmol/l for free $Zn^{2+}$.

**Figure 2. p62 is not required for Keap1 to sense $Zn^{2+}$.**

**A** & **B**, EGFP-mKeap1 (Keap1) or a mutated form that lacks His-225, Cys-226, and Cys-613 ($Keap1^{HCC}$) were expressed in COS1 cells and left untreated or treated with $ZnCl_2$

(Zn) (*A*) or $CdCl_2$ (Cd), sodium arsenite (As), or sodium selenite (Se) (*B*). **C**, COS1 cells expressing EGFP-mKeap1 were treated with ($+Zn^{2+}$) or without ($-Zn^{2+}$) $ZnCl_2$ for 2 h and cells were fixed, permeabilized and probed for endogenous p62 and DNA. Images show signals for EGFP-mKeap1, p62, and DNA (TO-PRO-3). Scale-bar = 25 μm. **D**, wt or *p62*$^{-/-}$ MEF cells were treated with the indicated concentrations of zinc-pyrithione (ZnPy) complexes for 2 h. Lysates were blotted for endogenous mNrf2, Keap1, and p62.

**Figure 3.** T**he CRL$^{Keap1}$ complex remains intact after triggering of its NO-, $Zn^{2+}$ or Alkenal sensors.**

**A** & **B**, The indicated combinations of proteins were transiently expressed in duplicate dishes of COS1 cells. The cells were either untreated (-) or treated for 2 h with Sul, tBHQ, Acro, or $CdCl_2$, and EGFP-tagged (*A*) proteins were immuno-precipitated. Alternatively (*B*) *in vivo* formaldehyde cross-linking of proteins was performed, followed by pull-down of his-tagged material. Input, IP and pull-down samples were blotted with the indicated antibodies. **C**, mNrf2$^{\Delta 17\text{-}32}$-V5 was expressed in COS1 cells either alone (-EGFP-mKeap1) or with EGFP-mKeap1 (+EGFP-mKeap1). Cytochemistry was performed upon untreated cells (-) or those exposed to Sul, tBHQ, Acro, or $Cd^{2+}$ for 2 h. Scale bar = 10 μm.

**Figure 4. Nrf2 constitutively associates with mKeap1.**

**A**, Wild-type *Keap1*$^{+/+}$ (wt) or knockout *Keap1*$^{-/-}$ (k) mouse fibroblasts were left untreated (-) or were treated for 2 h with MG132, Sul, tBHQ, Acro, or $Cd^{2+}$. Keap1 was immunoprecipitated and the input and immuno-precipitates (IP) were blotted with the

indicated antibodies. The band that represents Keap1 is indicated by an asterisk. **B**, Duplicate dishes of wt *Nrf2*$^{+/+}$ or *Nrf2*$^{-/-}$ primary MEF cells were left untreated (-) or were treated with MG132 or Sul for 2 h before immunoblotting for endogenous mNrf2 (horizontal arrow). The position of the putative Neh2-β-gal fusion protein that is expressed in *Nrf2*$^{-/-}$ fibroblasts as a consequence of the Nrf2 targeting strategy (Itoh et al., 1997) is indicated by a hash symbol. Std = 0.3 ng recombinant his-tagged mNrf2. Molecular-weight markers are indicated to the left of the blot. **C**, Immunocytochemical detection of endogenous mNrf2 was performed on wt *Nrf2*$^{+/+}$ or *Nrf2*$^{-/-}$ primary MEF cells that were untreated (-) or treated for 2 h with MG132 or Sul. Micrographs display the Alexa-fluor 568 signal originating with the anti-Nrf2 antibody. Scale bar = 10 μm.

**Figure 5. mKeap1 levels are not significantly reduced in stressed cells.**

**A**, Wild-type *Keap1*$^{+/+}$ (wt) or knockout *Keap1*$^{-/-}$ (k) immortalised MEF cells were left untreated or were treated with Sul, tBHQ, Acro, or $CdCl_2$ for 2 h. Lysates were blotted for endogenous mNrf2 or mKeap1. The asterisk indicates the position of mKeap1 protein. **B**, Immortalised *Keap1*$^{-/-}$ MEF cells were treated with CHX. Western-blotting for mKeap1 was performed at different CHX-chase time points. The graph depicts the logarithm of the relative abundance of mKeap1 protein as a function of CHX-chase time (mean of three independent experiments.) The best-fit-line with 95% confidence intervals and the derived half-live are presented. **C** & **D**, The indicated combinations of proteins were transiently expressed in duplicate dishes of COS1 cells. The cells were left untreated or were treated for 2 h with Sul, tBHQ, Acro, or $Cd^{2+}$ and EGFP-tagged (*C*) proteins were immuno-precipitated. Alternatively (*D*) *in vivo* formaldehyde cross-linking

of proteins was performed, followed by pull-down of his-tagged material. Input, IP and pull-down samples were blotted with the indicated antibodies.

**Figure 6. The Keap1 and Cul3 proteins physically associate even in stressed cells**. The indicated combinations of proteins were transiently expressed in duplicate dishes of COS1 cells. The cells were left untreated (-) or were treated for 2 h with Sul, tBHQ, Acro, or $Cd^{2+}$ and ECFP-tagged (*A* & *C*) proteins were immuno-precipitated. Alternatively (*B*) *in vivo* formaldehyde cross-linking of proteins was performed, followed by pull-down of his-tagged material. Input, IP and pull-down samples were blotted with the indicated antibodiesn.

**Figure 7. Triggering the $Zn^{2+}$ Sensor elicits a conformational change in mKeap1.** **A** – **F**, the FRET efficiency displayed by Keap1FRET, or variants thereof, was measured in COS1 cells before (control) or 30 min post-treatment with the indicated chemicals (Sul (*A*), 4HNE (*B*), $ZnCl_2$ (*C*), $CdCl_2$ (*D*), $NaAsO_2$ (*E*), or $Na_2SeO_3$ (*F*)). Data are presented as mean ± SEM (*A*, *C*, & *E*: n = 111 – 120 cells collected over three independent biological experiments performed on separate occasions; *B*, *D* & *F*) n = 78 – 80 cells collected over two independent biological experiments performed on separate occasions). Data were analysed by two-way ANOVA with a Bonferroni post-test. *, $P < 0.001$.

**Table 1. Chemicals, vehicles, and final concentrations, used during the course of this study**. All chemicals are potent activators of Nrf2 at the concentrations stipulated for both cell models (McMahon et al., 2010) . ND: Not done.

939

940

941

**Table_1**

| | Vehicle | Stock Concentration | Final Concentration (COS1 Cells) | Final Concentration (MEF Cells) |
|---|---|---|---|---|
| **Sulforaphane** | DMSO | 15 mM | 15 μM | 15 μM |
| **tBHQ** | DMSO | 300 mM | 300 μM | 100 μM |
| **Acrolein** | Ethanol | 100 mM | 100 μM | 33 μM |
| **4-hydroxynonenal** | Ethanol | 64 mM | 64 μM | ND |
| **Cadmium chloride** | MilliQ water | 100 mM | 45 μM | 45 μM |
| **Sodium Arsenite** | MilliQ water | 100 mM | 15 μM | ND |
| **Sodium selenite** | MilliQ water | 100 mM | 5 μM | ND |
| **Zinc chloride** | MilliQ water | 150 mM | 150 μM | Various - see text |
| **Pyrithione** | MilliQ water | 60 mM | ND | ND |
| **Cycloheximide** | DMSO | 40 mg/ml | ND | 40 μg/ml |
| **MG-132** | DMSO | 10 mM | 10 μM | 10 μM |

Figure_1
Click here to download high resolution image

# Figure 1

**A**

| | NO Sensor | $Zn^{2+}$ Sensor | Alkenal Sensor |
|---|---|---|---|
| PRIMARY: Endogenous 'danger' signals | NO (20 µM) | $Zn^{2+}$ (150 µM) | 4HNE (66 µM) |
| | | | Acro (100 µM) |
| SECONDARY: Common environmental toxins | tBHQ (300 µM) | $As^{3+}$ (15 µM) | |
| | Sul (15 µM) | | |
| TERTIARY: Molecular Mimicry | | $Cd^{2+}$ (45 µM) | |
| | | $Se^{4+}$ (5 µM) | |

**B**

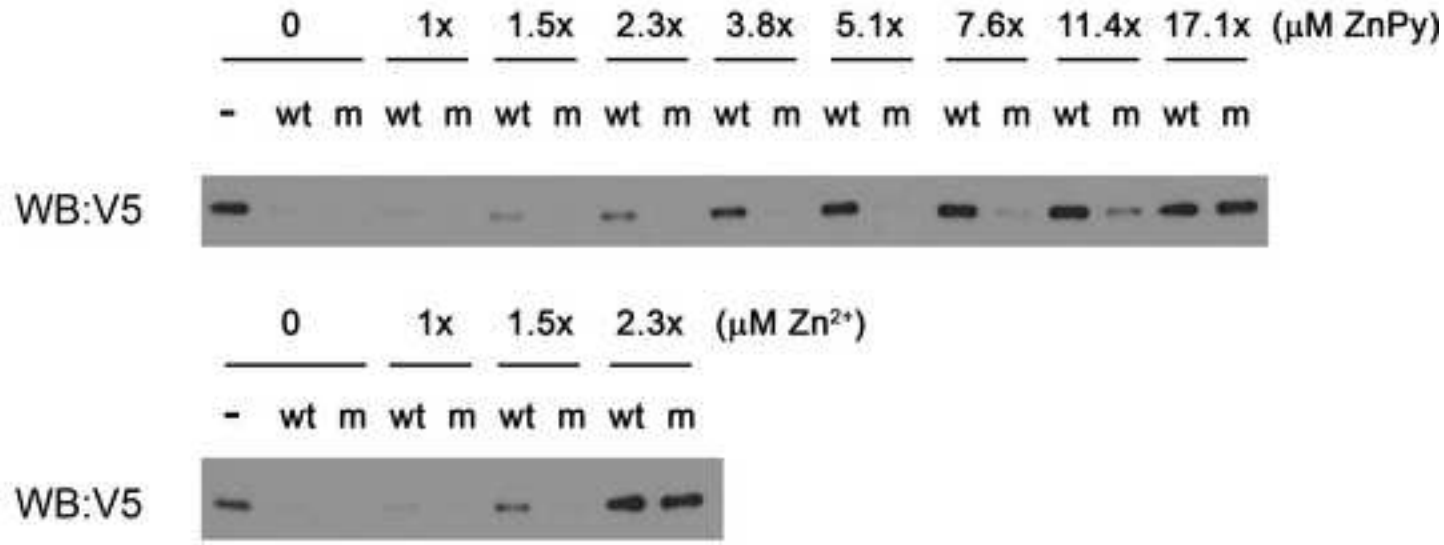

Figure_2
Click here to download high resolution image

# Figure 2

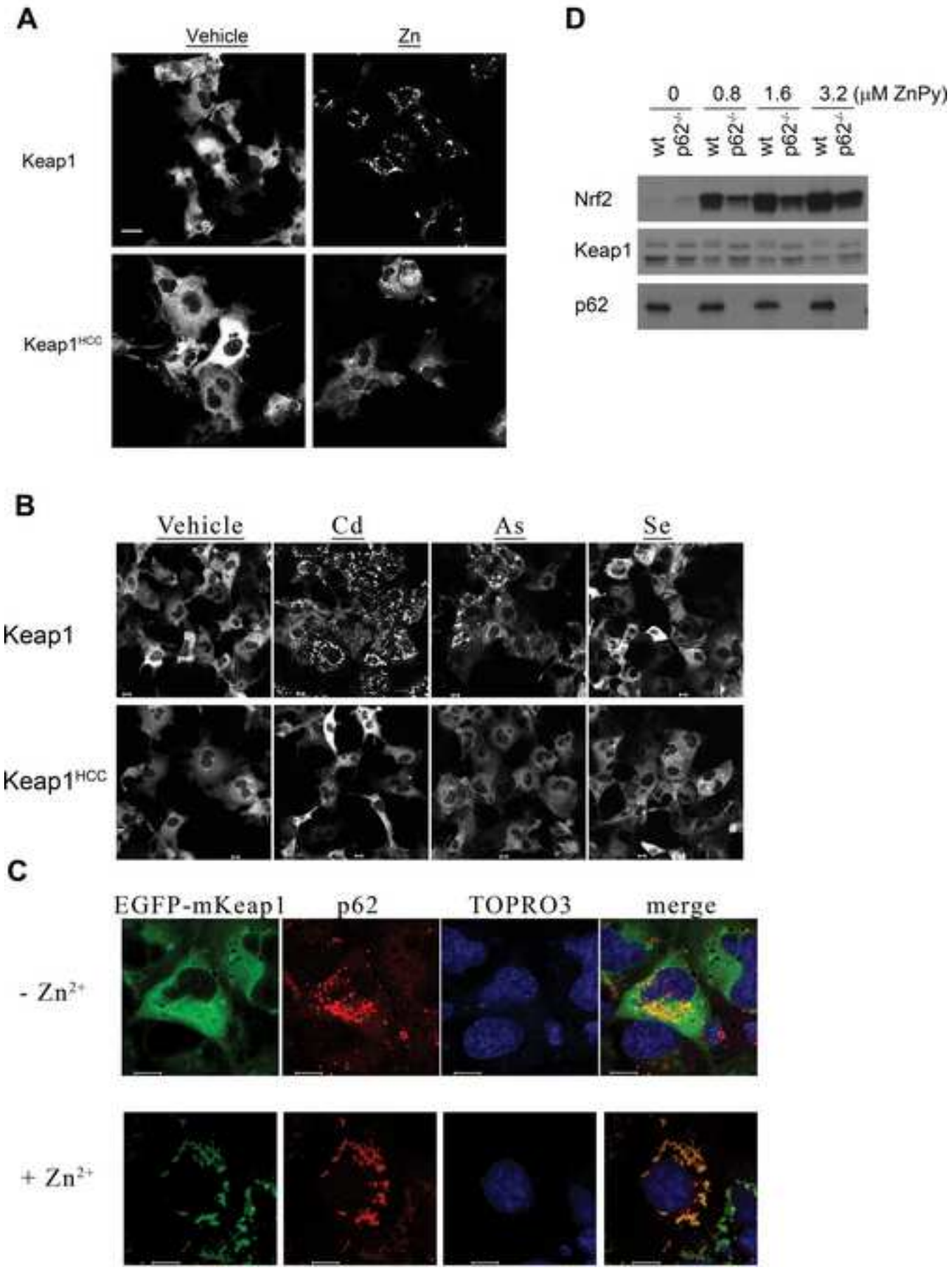

Figure_3
Click here to download high resolution image

# Figure 3

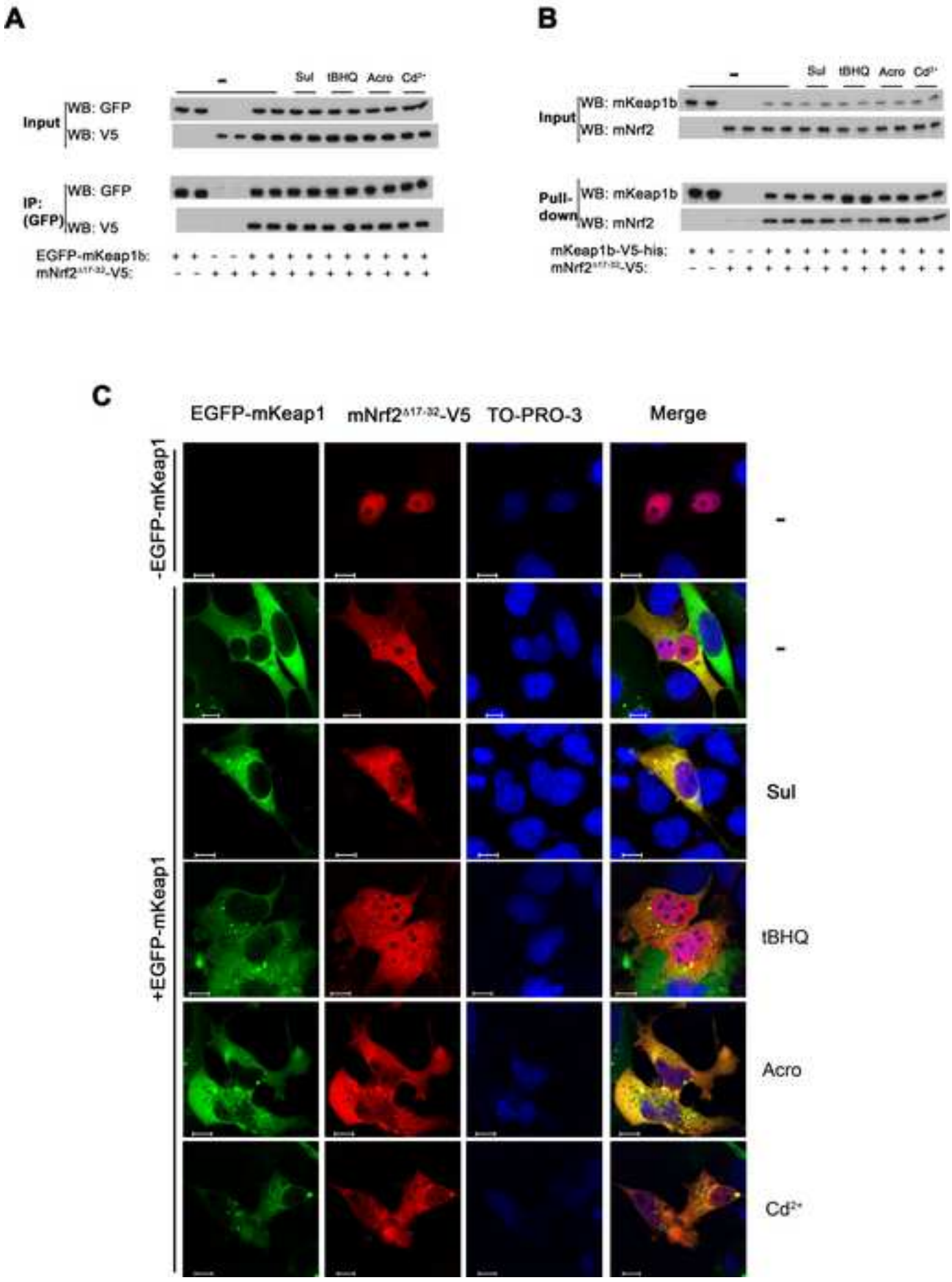

Figure_4
Click here to download high resolution image

# Figure 4

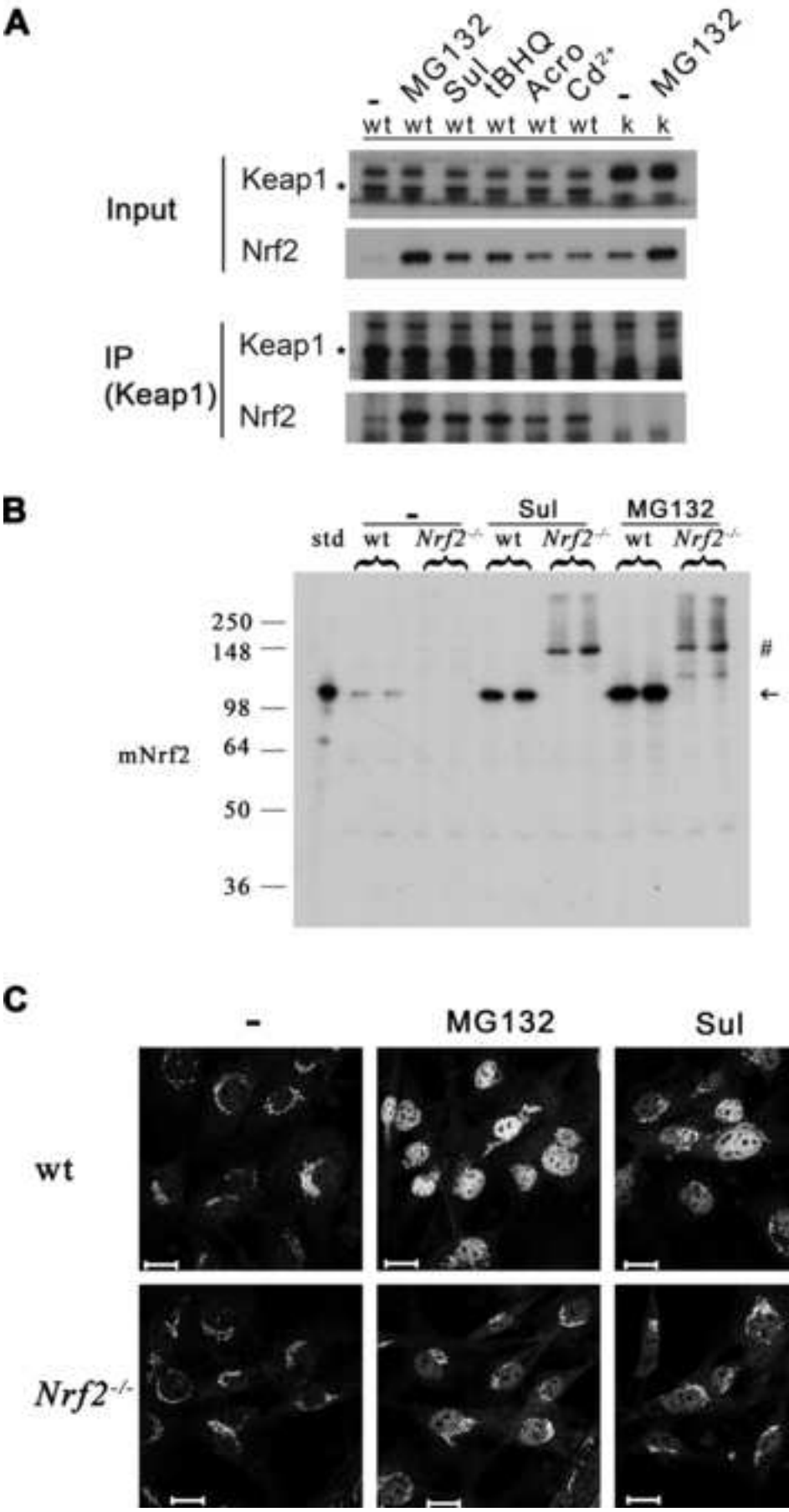

Figure_5
Click here to download high resolution image

# Figure 5

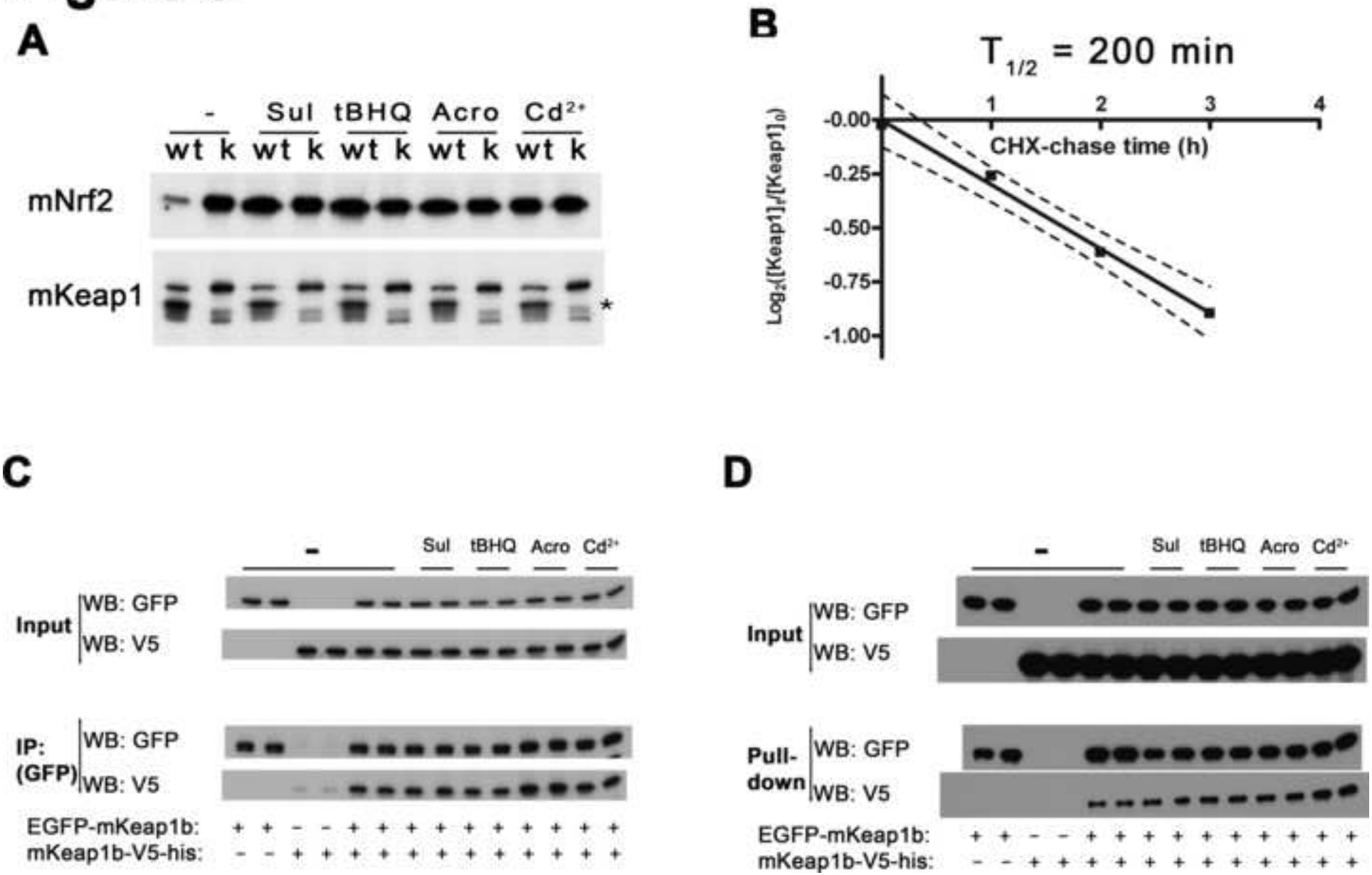

Figure_6
Click here to download high resolution image

# Figure 6

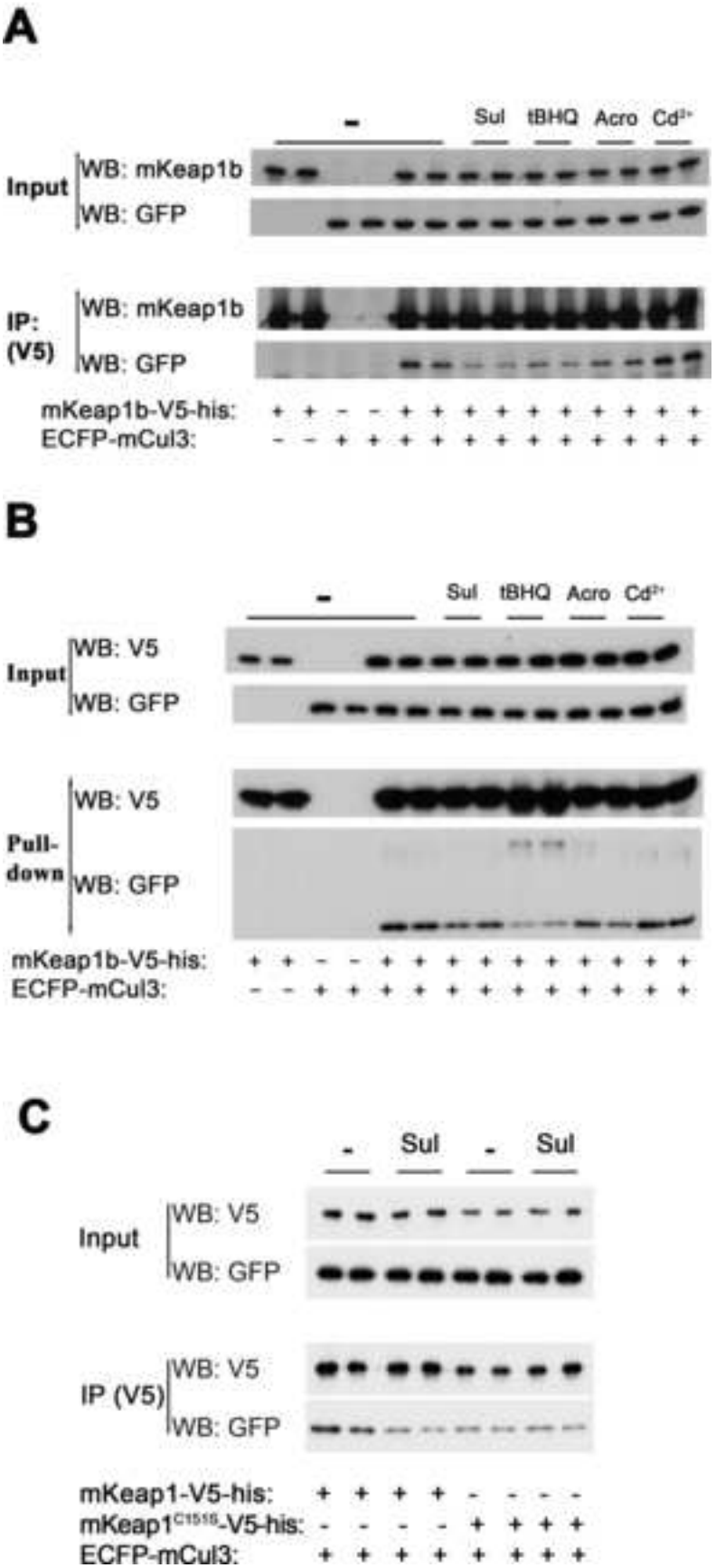

Figure_7
Click here to download high resolution image

# Figure 7

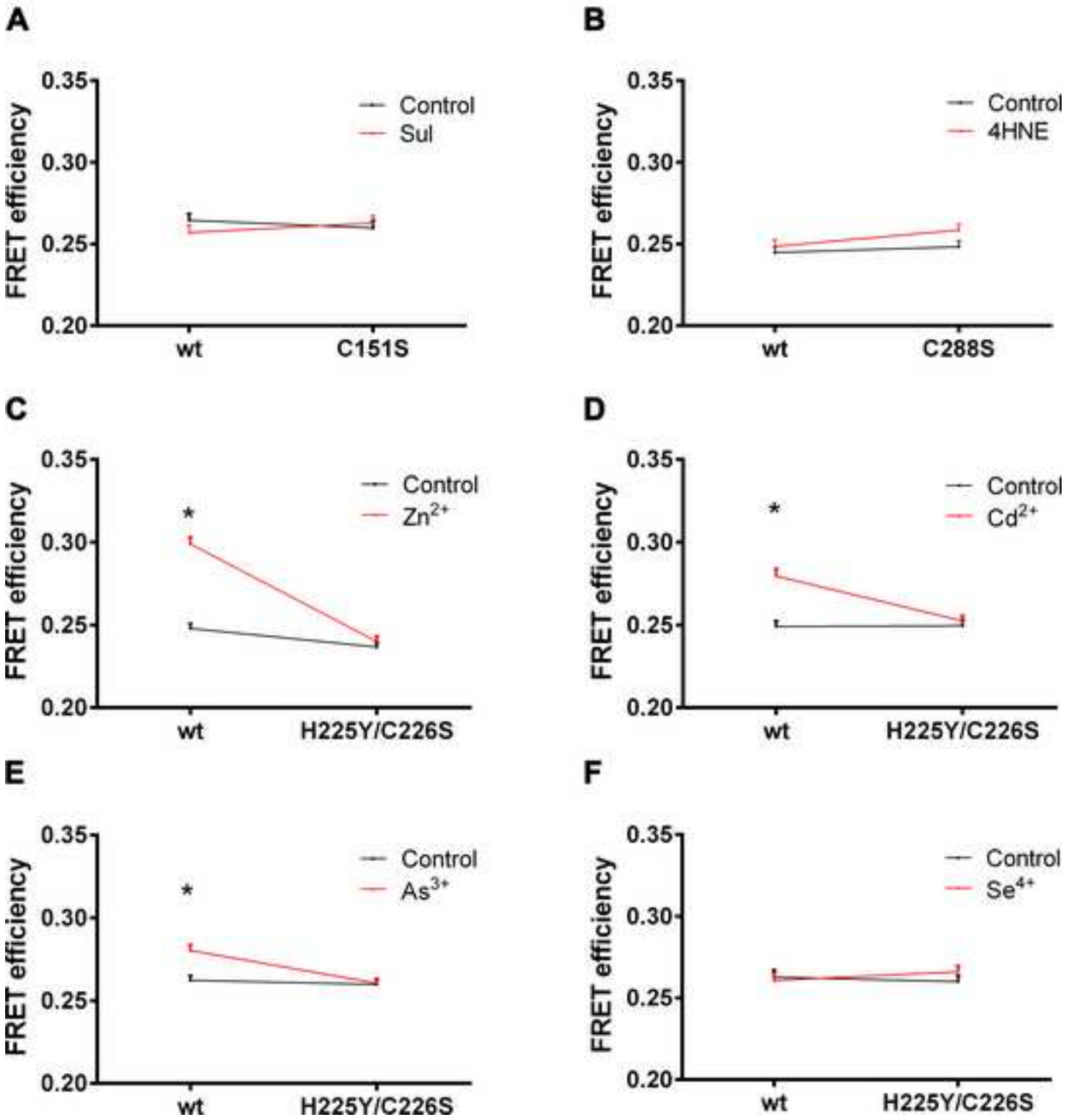

**Supplementary Text**

**Click here to download Supplementary Material: SUPPLEMENTAL INFORMATION_v2.doc**

**Supplementary Figure_1**

**Click here to download Supplementary Material: FIGURE_S1.tif**

**Supplementary Figure_2**

**Click here to download Supplementary Material: FIGURE_S2.tif**

**Supplementary Figure_3**

**Click here to download Supplementary Material: FIGURE_S3.tif**

**Supplementary Figure 4**

**Click here to download Supplementary Material: FIGURE_S4.tif**

***Conflict of Interest form (from all the authors)**

**Click here to download Conflict of Interest form (from all the authors): coi_disclosure_MMM.pdf**

***Conflict of Interest form (from all the authors)**

**Click here to download Conflict of Interest form (from all the authors): coi_disclosure_SS.pdf**

***Conflict of Interest form (from all the authors)**

**Click here to download Conflict of Interest form (from all the authors): coi_disclosure_jdh.pdf**

***Conflict of Interest Statement**

**Click here to download Conflict of Interest Statement: Conflict_of_Interest_Statement.docx**

**Manuscript Track-changed**

**Click here to download Supplementary Material: MANUSCRIPT_v2_TRACK-CHANGED.pdf**